# UNDERSTANDING THE ROLE OF THE GENES EOMESODERMIN, INTERLEUKIN-6 AND SOX17 IN THE PRE-GASTRULATION PIG EMBRYO

**By**

**Liam Wood, BSc**

**Thesis submitted to the University of Nottingham for the degree of Master of Research**

**September 2018**




**Division of Animal Sciences**
**School of Biosciences**
**University of Nottingham**
**Sutton Bonington**
**United Kingdom**

## Abstract

The mechanisms of early embryonic development in large mammals is still largely unknown. These mechanisms have been well defined in the mouse embryo. However, recent literature has found striking differences between early development in mice and larger mammals such as humans, pigs and monkeys. Since human embryos cannot be used for ethical reasons, porcine embryos were used in to establish a model of early development in large mammals. In this thesis I sought to investigate the roles of 2 genes, Interleukin-6 (IL-6) and Eomesodermin (EOMES), in the early development of the pig embryo. These genes were chosen due to preliminary data which highlights different expression patterns between mice and pigs. Based on this I drew the hypothesis that the function of IL-6 and EOMES in the pig embryo differs to that of the mouse embryo. To gain an insight into the role of IL-6, porcine embryos were cultured in the presence of IL-6 and an IL-6 inhibitor. A method of IL-6 knockout by CRISPR-Cas9 genome editing was also developed. Considering that EOMES expression in the embryo is outside the scope of *in vitro* study a CRISPR based method was designed with a view of generating high knockout efficiencies prior to an *in vivo* study. The study found that IL-6 has a trophic effect on the trophectoderm lineage of *in vitro* parthenogenetically activated pig embryos, but does not play a role in pluripotency as hypothesised. Additionally Leukaemia inhibitory factor has a negative effect on the expansion of the trophectoderm lineage *in vitro*. Furthermore, genome editing via CRISPR-Cas9 methods were somewhat efficient at creating EOMES-null embryos, however, further optimisation is required in order to increase editing efficiency for future studies.

**ACKNOWLEDGMENTS**

Firstly, I would like to thank my supervisor Dr Ramiro Alberio for his guidance and supervision throughout my project. I would also like to thank Doris Klisch, Lydia Kwong, and the rest of the technical team for all their help and advice they have offered throughout. I would like to thank Qifan Zhu and Priscila Ramos-Ibeas for the encouragement and help they have provided me with throughout our experiments.

# Contents

Abstract ..... 2
1. Introduction ..... 8
1.1.1 Development in the preimplantation embryo – Blastulation ..... 8
1.1.2 Development in the preimplantation embryo – Gastrulation ..... 10
1.2 Interleukin-6 cytokine family in the embryo ..... 13
1.2.1 JAK/STAT signalling in the embryo ..... 14
1.2.2 Interleukin-6 cytokine family and pluripotency ..... 14
1.3 The T-Box transcription factors in early development ..... 15
1.3.1 Eomesodermin and epithelial to mesenchymal transition ..... 16
1.3.2 Eomes in the mesoderm ..... 16
1.3.3 Eomes in the Visceral Endoderm and Axis formation. ..... 17
1.3.4 Eomes in the Definitive Endoderm ..... 18
1.3.5 Eomes in Germ Cells ..... 19
1.3.6 Eomes in trophectoderm ..... 19
1.4. The Sry-Box protein family in early development ..... 20
1.4.1 Sox17 in the definitive endoderm ..... 20
1.4.2 Sox17 in PGCs ..... 21
1.5 Hypothesis and aims ..... 23
2. Materials and methods: ..... 25
2.1 Oocyte collection: ..... 25
2.2 Parthenogenetic activation and blastocyst generation: ..... 26
2.3 Guide RNA synthesis and preparation: ..... 28
2.4 Porcine oocyte microinjection ..... 28
2.5 DNA extraction and genotyping ..... 28
2.6 Immunofluorescence staining of blastocysts ..... 31
2.7 Embryo treatments and inhibition: ..... 32
3. Interleukin-6 Results ..... 33
3.1 IL-6 family expression in the preimplantation embryo: ..... 33
3.2 IL-6 Supplementation and inhibition on *in vitro* embryos ..... 34
3.3 IL-6 Supplementation and inhibition on *in vivo* embryos ..... 38
3.4 IL-6 Knockout Experiments ..... 41
3.5 Conclusions ..... 44
4. Eomesodermin Results ..... 46
Conclusions ..... 51
5. Discussion ..... 53
5.1 Understanding the role of Interleukin-6 in the developing pig embryo ..... 53
5.2 Understanding the role of EOMES in the gastrulating pig embryo ..... 56

5.3 Conclusions ..... 59
5.4 Future work ..... 60
6. References ..... 61

# Figures and Tables

## List of tables:


Table 1: Search medium recipe 25
Table 2: In vitro maturation medium recipe 26
Table 3: Porcine zygote medium recipe 27
Table 4: Activation medium recipe 27
Table 5: N2B27 medium recipe 27
Table 6: List of primers used for genes studied 29
Table 7: F1R2 PCR mix 29
Table 8: F1R1 PCR mix 29
Table 9: F2R2 PCR mix 29
Table 10: First PCR mix for IL6 fragment with proofreading KAPA polymerase 30
Table 11: Second PCR mix for IL6 fragment 30
Table 12: Polyacrylamide gel recipe 30
Table 13: Antibodies and dilutions 31
Table 14: Embryo treatments and concentrations 32


## List of figures:


Figure 1: Structure of early and late blastocyst 9
Figure 2: Comparison of morphology between gastrulating mouse and pig embryos 11
Figure 3: Diagram of LIF and hypothesised IL6 signalling in the embryo 15
Figure 4: Expression plots of IL-6 cytokine family in the early embryo 33
Figure 5: Brightfield images of treated pig blastocysts 34
Figure 6: Immunofluorescence staining images from treatment groups 35
Figure 7: Number of cells in treated embryos 36
Figure 8: ICM:TE ratio percentage of blastocyst groups 37
Figure 9: Quantification of NANOG and SOX17 positive cells in parthenote embryos 37
Figure 10: Brightfield images of E7 blastocysts 38
Figure 11: Immunofluorescence staining images from treatment groups 39
Figure 12: Number of cells in treated *in vivo* embryos 39
Figure 13: ICM:TE ratio percentage of blastocyst groups 40
Figure 14: Quantification of NANOG and SOX17 positive cells in *in vivo* embryos 40
Figure 15: Annotated diagram of IL-6 target sequence 41
Figure 16: Heteroduplex PAGE analysis of presumptive edited blastocysts 42
Figure 17: Comparison of edited and control blastocysts 43
Figure 18: Expression plots of PS and mesodermal markers in pig embryos 47
Figure 19: Annotated sequence of EOMES exon 1 48
Figure 20: Heteroduplex PAGE analysis of guide 1 injected blastocysts 48
Figure 21: Representative indels from guide 1 knockout embryos 49
Figure 22: Comparison of mutations found in guide 1 injected pig embryos 49
Figure 23: Mean blastocyst development rates 50

## List of abbreviations

| | |
|---|---|
| AP | Anterior-Posterior |
| AVE | Anterior visceral endoderm |
| BMP | Bone morphogenetic protein |
| Cdx2 | Caudal type homeobox 2 |
| DMAP | Dimethylaminopurine |
| DVE | Distal visceral endoderm |
| E | Embryonic day |
| EMT | Epithelial to mesenchymal transition |
| EOMES | Eomesodermin |
| Epi | Epiblast |
| ESCs | Embryonic stem cells |
| FGF | Fibroblast growth factor |
| hPGCLC | Human PGC like cells |
| Hypo | Hypoblast |
| ICM | Inner cell mass |
| IF | Immunofluorescence |
| IL6 | Interleukin 6 |
| IL6R | Interleukin 6 receptor |
| IL6ST | Interleukin 6 signal transducer |
| iMeLC | Incipient mesoderm like cell |
| JAK | Janus Kinase |
| LIF | Leukaemia inhibitory factor |
| LIFR | Leukaemia inhibitory factor receptor |
| MAPK | Mitogen activated protein kinases |
| PAM | Protospacer adjuster motif |
| PGC | Primordial germ cell |
| RPKM | Reads per kilobase of transcript per million mapped reads |
| scRNAseq | Single cell RNA sequencing |
| STAT | Signal transducer and activator of transcription |
| T | Brachyury |
| TE | Trophectoderm |
| TGFβ | Transforming growth factor beta |
| VE | Visceral endoderm |

# 1. Introduction

### 1.1.1 Development in the preimplantation embryo – Blastulation

The diversity of animal tissue morphology and function is decided in the very first stages of embryogenesis. After a series of programmed cell divisions the multicellular blastula, or blastocyst in mammals, is formed, in which groups of cells have their fate specified (Ip and Gridley, 2002). In preparation for implantation the embryo undergoes a series of morphological changes prior to entering the uterus. The single cell zygote first undergoes a series of divisions to become a totipotent 8-cell embryo. The embryo then undergoes a process termed compaction, where multiple morphological changes occur, mainly to establish cell adhesion and organisation within the embryo, which causes the embryo to become polarised (Menchero et al, 2016; Ziomek and Johnson, 1980). Within the polarised embryo the outer polarised cells will eventually give rise to the trophectoderm (TE), whereas the inner apolar cells form the inner cell mass (ICM) (Chazaud et al, 2006). The cells then undergo 2 further divisions upon which the blastocoel (a fluid filled cavity within the embryo) forms at the 32-cell stage. This process termed cavitation places physical stress on the blastomeres, causing deformation of the cells and leading to formation of the ICM as the cells are forced to one end of the embryo. (Menchero et al, 2016). At this point there are two distinct cell populations within the embryo, the ICM and the surrounding layer of TE, a layer of epithelial cells which gives rise to extraembryonic tissues and is the precursor to the placenta. From this point the ICM separates into two distinct cell types, the epiblast which is the precursor of the embryo proper and the tissues that form the body, and the hypoblast/primitive endoderm. The hypoblast is localised beneath the epiblast, encapsulating it within a layer of hypoblast/TE. In mouse embryos the TE also develops into two types of cell, polar cells in contact with the ICM which proliferate, and giant trophoblastic cells which invade the endometrium to facilitate implantation.

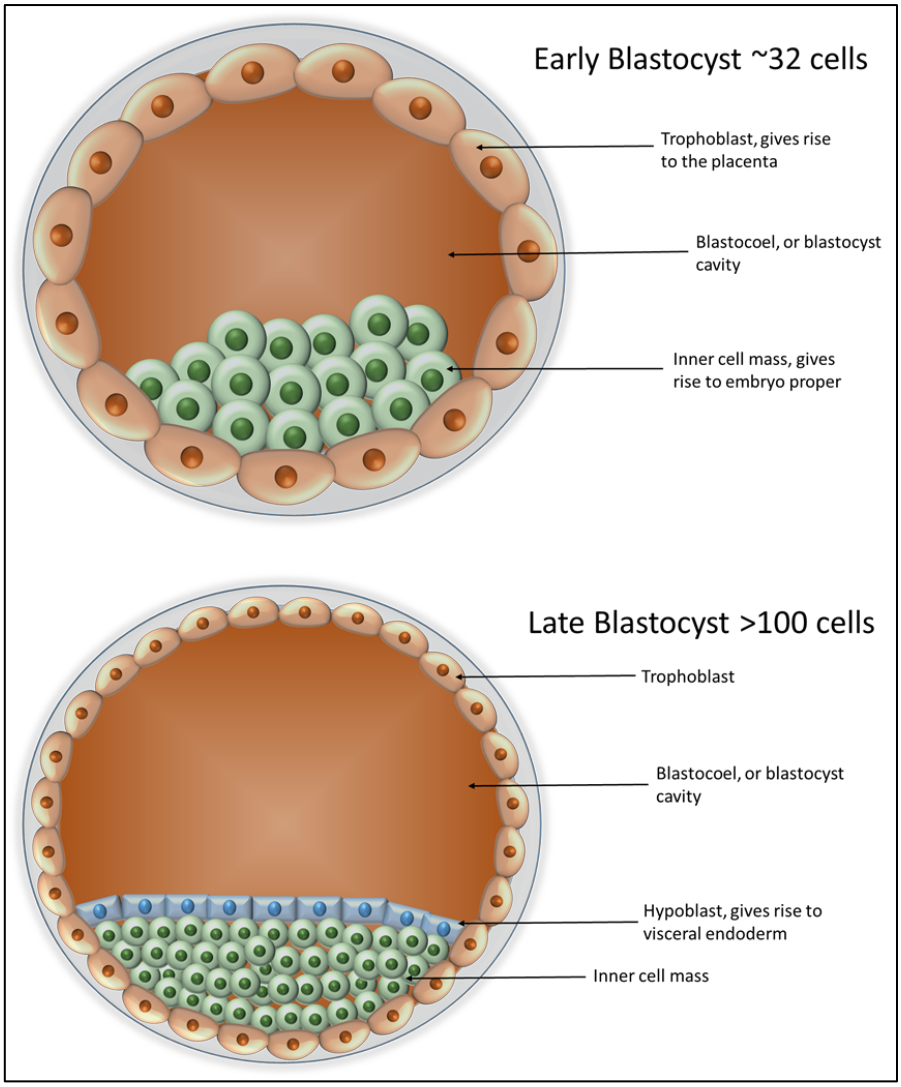



*Figure 1 - structure of early and late blastocyst*

The emergence of these distinct cell populations within the preimplantation embryo is regulated by a web of transcription factors, which determines the commitment to a specific lineage. The main determining factor of the TE lineage in mice is Caudal-type homeobox factor 2 (Cdx2), with other transcription factors such as GATA3 and Eomesodermin (Eomes) also linked to TE lineage segregation (Home et al, 2009). Expression of Oct4, Sox2 and Nanog are crucial for ICM formation in the mouse embryo, with Sox2 being the earliest ICM marker with increased expression in apolar cells at the 16 cell stage (Wicklow et al, 2014). Expression of these factors is mostly ubiquitous in blastomeres until late blastocyst stage where they become restricted to their respective lineage. A study has shown reciprocal inhibition between OCT4 and Cdx2 to cause lineage segregation in embryonic stem cells (ESCs), indicating that this may also be the case in the preimplantation embryo (Menchero et al, 2016). In addition, the Hippo pathway has been shown to be involved in the first lineage

choice, via the downstream effectors Yap and Tead4, which are upstream regulators of Cdx2, and therefore essential for TE formation (Posfai et al, 2017). Other signalling pathways implicated in this lineage decision is Tyrosine kinase signalling which plays a role in both TE/ICM segregation and epiblast/hypoblast lineage fate in mice, and LIF signalling is implicated in the formation of the TE via JAK/Stat signalling but the exact mechanism of this signalling pathway is yet to be explored. (Menchero et al, 2016).

The segregation of epiblast and hypoblast is decided in the blastocyst stage. The transcription factors Nanog and Gata6 are co-expressed in the morula but expression of one of these factors resides randomly in the ICM cells causing a salt and pepper distribution of NANOG or GATA6 positive cells, which gives rise to the epiblast or hypoblast respectively (Menchero et al, 2016, Chazaud et al, 2006). The lineage segregation of epiblast and hypoblast is controlled by propagation of MAPK signalling pathway by FGF. In the mouse embryo MAPK activates Gata6 and represses Nanog to form hypoblast, whereas in the bovine embryo MAPK inhibits Nanog but does not induce expression of Gata6, leading to only partial inhibition of hypoblast when MAPK is blocked. This study highlights differences in lineage segregation between mice and larger mammals as early as the blastocyst stage (Kuijk et al, 2012).

### 1.1.2 Development in the preimplantation embryo – Gastrulation

After the second lineage specification of ICM into epiblast and hypoblast, the epiblast is further specified to form the embryonic germ layers. This process, termed gastrulation, is a mechanism in which epiblast cells collectively migrate, change morphology and rearrange in a coordinated manner to form three distinct germ layers (Solnica-Krezel and Sepich, 2012; Keller, 2005). The function of the three types of germ layers is conserved across all vertebrates; the ectoderm gives rise to a number of tissues and organs including skin, hair, brain, spinal cord and nervous tissue. The mesoderm forms the heart, muscle, bones and blood, and the endoderm gives rise to the gut, pancreas, liver and epithelial tissues in the lungs (Stemple, 2001; Swarr and Morrisey, 2015). This process is initiated alongside the formation of the primary internalisation site, known as the primitive streak in mammals and birds, or the blastopore lip in reptiles (Stower and Bertocchini, 2017). The beginning of gastrulation marks the point at which the topographic arrangement of mammalian embryos begins to vary considerably between species, with the mouse embryo forming a large cylindrical shape and the rabbit, primate, pig and human embryo forming a smaller flat disc shape, typical of most mammals. (Hassoun et al, 2009). These anatomical differences

between mammalian embryos have not been appreciated until recently due to limited information on the embryology of larger mammals. Despite the striking morphological differences between rodent and other mammalian embryos, the mouse embryo remains the most utilised model for early developmental studies due to convenience, similar implantation schedule to humans and advanced genetics (Hassoun et al, 2009; Rodda et al, 2005). Therefore, studies on murine embryos may only be partially compared to flat disc embryos in terms of molecular processes and topography, and careful consideration should be taken into account when making comparisons (Hassoun et al, 2009).

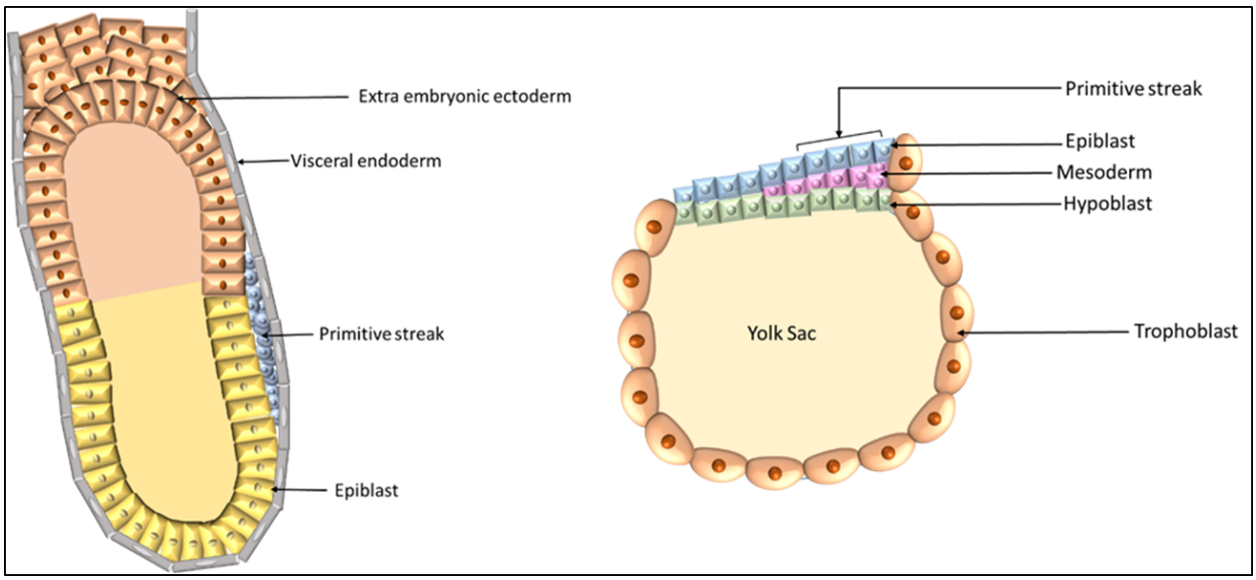



*Figure 2 - Comparison between the morphology of the gastrulating mouse embryo (left) and the gastrulating pig embryo (right)*

Prior to gastrulation, the pluripotent epiblast expands and becomes primed for differentiation. The shift from naïve to primed state is marked by a metabolic shift in the epiblast to increase proliferation and epigenetic remodelling in preparation for differentiation during gastrulation (Ramos-Ibeas et al, 2018). Primed pluripotency in the pig epiblast markedly differs from that of the mouse. Expression patterns of key pluripotency factors OCT4 and NANOG are present in all pluripotent stages as is the case in the mouse epiblast. However there are differences in expression patterns of many other pluripotency genes including Nanog KLF4 and TBX3 (Ramos-Ibeas et al, 2018), highlighting further key differences between the embryogenesis of mice and larger mammals.

The anterior-posterior axis of the mammalian embryo is established just prior to gastrulation. In order for the primitive streak to be established, formation of this asymmetry in the epiblast and visceral endoderm is required, and marks the onset of gastrulation (Zernicka-Goetz, 2002; Tam and Loebel, 2007). The primitive streak is a localised region within the epiblast of the mammalian embryo, which serves as a site of internalisation, where epiblast cells migrate through the primitive streak to form the underlying mesendoderm (Rivera-Pérez and Magnuson, 2005). In order for the primitive streak to form, the epiblast is specified in response to Wnt3 in response to Nodal and potentially BMP4 from the extraembryonic ectoderm (Mohamed, Clarke and Dufort, 2004; Ben-Haim et al, 2006). In addition, the initiation of streak formation is marked by Brachyury (T) expression in certain cells within the epiblast (Rivera-Pérez and Magnuson, 2005). The mesoderm/endoderm marker gene Eomesodermin (Eomes) is also expressed in the epiblast and nascent mesoderm of the mouse embryo at this stage (Arnold, 2008).

Ingression of the epiblast to form mesendoderm occurs when the epiblast reaches a critical number of cells (Tam and Behringer, 1997). To do so, the cells must undergo epithelial to mesenchymal transition (EMT), with the mesenchymal cells migrating through the primitive streak to form the mesendoderm. Nodal and Mixl1 are essential for mesoderm patterning in the mouse, as well as BMP4 which is essential for expression of the mesodermal marker T (Winnier et al, 1995; Hart et al, 2002). The formation of either mesoderm or endoderm is dependent on levels of Nodal and Wnt in the primitive streak (Gadue et al, 2006).

Primordial germ cells (PGCs), are the precursors to spermatozoa and oocytes, and derive from a founder population of epiblast cells, within a region that mainly gives rise to mesoderm (Lawson et al, 1999). Mouse PGCs migrate through the primitive streak in early gastrulation, then migrate through the developing endoderm and colonise the genital ridges. Bmp4 is essential for PGC specification as it is the upstream regulator of 2 transcription factors responsible for PGC survival and proliferation, Blimp1 and Prdm14 (Saitou and Yamaji, 2012). Recent work in our laboratory has demonstrated fundamental differences in the mechanisms of PGC specification between mice and larger mammals such as pigs and humans. Porcine PGCs originate not from a founder population, but from primitive streak competent epiblast cells by expression of BLIMP1 and SOX17, as a result of WNT and BMP rich environments (Kobayashi et al, 2017). This mechanism was also shown to be conserved in human and monkey PGC cell lines. In addition, PRDM14 may not be required for germ cell fate as it is in

mice. (Sugawa et al, 2015). These discrepancies between signalling pathways indicates that early development is not conserved between all mammals and that pigs may reflect more accurately the early development of humans. This also raises the question of other developmental pathways that may differ from the pathways already delineated in mice.

## 1.2 Interleukin-6 cytokine family in the embryo

Interleukins are a highly pleiotropic family of cytokines which have roles in many cellular processes, including but not limited to immune responses, bone and epithelial cell maintenance, tumour suppression and embryonic development. (Akdis et al, 2011).

Interleukin-6 (IL-6) was discovered as a result of high expression of the protein in virally infected fibroblasts (Content et al, 1982), and its role as a member of the interleukin family of cytokines was cemented after the discovery that transformed B cells respond to this peptide when produced by macrophages (Lee, 1992). One of the first studies to dissect the role of IL-6 in the developing embryo found murine blastocysts to express mRNA for IL-6 and Leukaemia Inhibitory Factor (LIF), a cytokine in the IL-6 family which has a similar function to IL-6 in terms of differentiation of immune cells, and also has the ability to maintain *in vitro* explants of murine ICM derived ESCs. Furthermore, mouse blastocysts were found to excrete both IL-6 and LIF *in vitro*, indicating that these molecules may mediate signalling between the pre-implantation blastocyst and the uterine wall. (Murray, Lee and Chiu, 1990). IL-6 transcripts are found at the 8-cell stage in mouse embryos, but not in fertilised oocytes or 2 cell embryos (Gerwin et al, 1995). IL-6 and LIF RNA transcripts were also found in expanded mouse blastocysts (E3) isolated from the uterine horns, as well as from blastocysts developed in vitro from the 2-cell stage. However, the functional proteins were only present after an additional day of *in vitro* culture, around the time of blastocyst hatching (E3.5 - 4) (Murray, Lee and Chiu, 1990).

To further elaborate upon the similarities between LIF and IL-6, the LIF receptor (LIFR) and IL-6 receptor (IL6R) both interact with gp130, the signal transducing component of the IL-6 receptor (otherwise known as IL6ST), as well as the G-CSF receptor, a receptor which cooperates with IL-6 to enhance Stat3 activation (Yan et al, 2013; Gearing et al, 1991).

### 1.2.1 JAK/STAT signalling in the embryo

The Janus kinase/signal transducer and activator of transcription, otherwise known as Jak/Stat, is a pleiotropic signalling cascade involved in many cellular functions, including cellular development, proliferation, differentiation, migration and apoptosis (Rawlings, Rosler and Harrison, 2004). This pathway is primarily initiated by engagement with cytokine-receptor complexes and mediates phosphorylation of downstream effectors. (Sansone and Bromberg, 2012)

Stat3 knockout embryos exhibit severe embryonic abnormalities. Up to E6, the only phenotypic abnormality was a stunted blastocyst outgrowth, but this did not contribute to embryonic lethality. The Stat3 deficient embryos were smaller than wildtype controls at the E6 egg cylinder stage and quickly degenerated prior to E7.5 with no mesoderm formation (Takeda et al, 1997). The degradation of the knockout embryos coincided with the wildtype expression of Stat3 in the visceral endoderm and decidua. Furthermore, inactivation of receptor molecules crucial for Stat3 activation such as LIFR and the IL-6 receptor domain gp130 also causes embryonic lethality, albeit less lethal, as LIFR deficient mice die shortly after birth and gp130 mice survive to E15.5-18.5 and terminate due to abnormalities in the mesoderm derived tissues (heart, placenta, blood) (Takeda et al, 1997).

### 1.2.2 Interleukin-6 cytokine family and pluripotency

LIF is vital for the maintenance of pluripotency in mouse embryonic cell lines derived from ICM explants of mouse embryos. LIF induces the dimerization of LIFR and gp130 to activate Stat3, which in turn activates the transcription factor Tfcp2I1, which activates the core pluripotency network by binding pluripotency factors necessary for self-renewal; Nanog, Sox2, Esrrb and Oct4 (Ohtsuka, Nakai-Futatsugi and Niwa, 2015; Papatsenko, Waghray and Lemischka, 2018).

Our most recent data highlights a stark contrast between the expression profiles of IL-6 and LIF in porcine and murine embryos. Single cell RNA-seq data showed that LIF is not expressed in the early pig embryo, and LIFR is expressed at very low levels between morula and E11 epiblast, which concurs with a previous study (Hall and Hyttel, 2014). Furthermore, our data shows that IL-6 is present in morulae and early blastocyst trophectoderm, whereas gp130 and IL6R are highly expressed in the ICM, but also present in the TE and epiblast. This is an

indication that IL-6 signals in a paracrine fashion and may play a crucial role in the maintenance of pluripotency in the ICM of the early pig embryo.

Considering the vital role LIF has in the preimplantation mouse embryo, it is striking that the preimplantation pig embryo does not express LIF at any stage. This raises the question of which, if any, cytokine fills the role of activating the JAK/STAT pathway and the core pluripotency network to maintain pluripotency within the embryo. The expression pattern of IL-6 suggests that this particular cytokine may carry out this role in the porcine embryo, highlighting a divergent mechanism in the maintenance of pluripotency from smaller mammals.

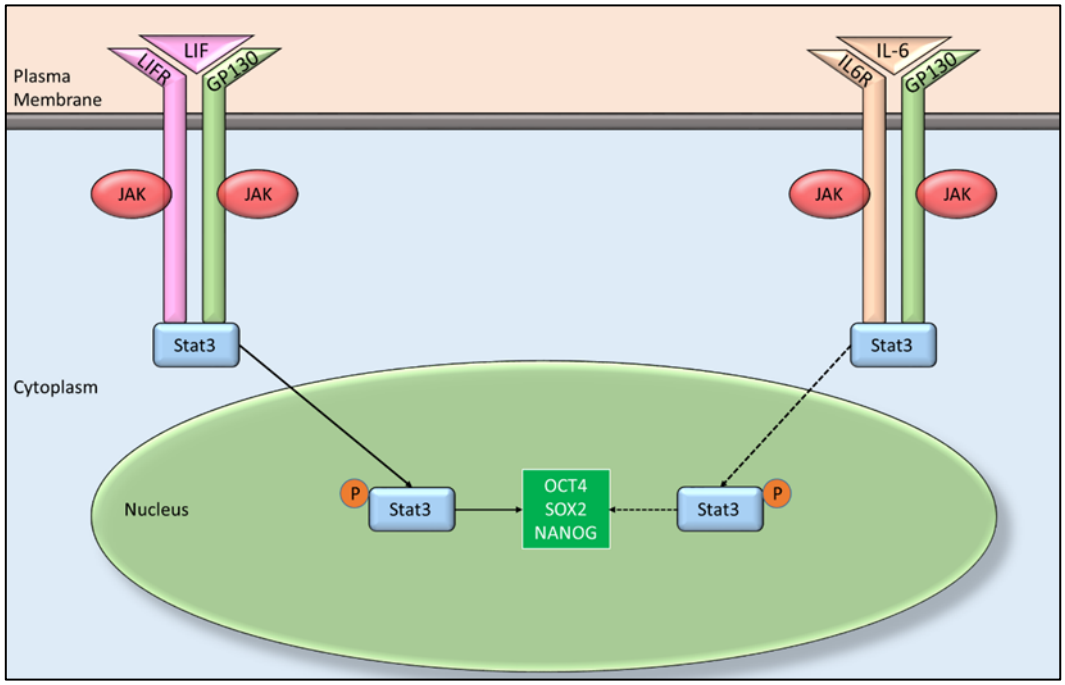



*Figure 3 - Diagram of LIF signalling to maintain pluripotency in the embryo. Depicted on the right is the hypothesised mechanism of induction of pluripotency mediated via IL-6 signalling.*

## 1.3 The T-Box transcription factors in early development

The T-box gene family is a group of transcription factors with a conserved DNA binding domain, also known as the T-box. The first discovered member of this family, brachyury, or T, was found to play a vital role in the development of the notochord and posterior mesoderm (Papaioannou, 2001). From this discovery a group of genes with pivotal roles in early embryonic development, cardiogenesis, limb development, and stem cell development was discovered (Papaioannou, 2014). The gene family can be divided into 5 subfamilies dependant on homology within the region encoding the T-box domain. The T-box transcription factors

have been shown to contain both activator and suppressor domains and also possess conserved and divergent transcriptional mechanisms which accounts for their differing roles in early development (Ouimette et al, 2010). The mechanisms of action of the T-box proteins can also be influenced by interactions with homeobox proteins and suppressor proteins. The proteins have also been shown to play a role in gene regulation via epigenetic modification (Papaioannou, 2014; Lu, Yang and Jin, 2011; Beisaw et al, 2017).

Eomesodermin (Eomes) is a member of the Tbr1 subfamily and plays a role in many aspects of development. Eomes has been shown to be expressed in the developing heart, brain and limbs, differentiating stem cells and also houses a plethora of roles in the early development of the embryo (Papaioannou, 2014).

### 1.3.1 Eomesodermin and epithelial to mesenchymal transition

Presence of Eomes in the epiblast is one of the earliest indicators of the onset of gastrulation. Eomes expression is first established in the posterior epiblast and extends into the primitive streak at E5.75 in mice (Costello et al, 2011). From the primitive streak Eomes expression extends into the nascent mesoderm where it induces mesodermal genes in a dose dependent manner (Arnold et al, 2008). During these early stages of development a significant proportion of epiblast cells transition from epithelial phenotype to mesenchyme, otherwise known as epithelial to mesenchymal transition (EMT) (Kerosuo and Bronner-Frasier, 2012). EMT is essential in the developing embryo to facilitate the migration of cells into the germ layers, and is achieved by the downregulation of adhesion junctions, cell polarity and rupture of the basement membrane (Kerosuo and Bronner-Frasier, 2012). In wildtype epiblast cells Fgf4 and Fgf8 are activated, which enables the expression of the downstream Snail to silence transcription of the adhesion protein E-Cadherin (Batlle et al, 2000), which in turn causes cell delamination and migration (Arnold et al, 2008). Interestingly, in Eomes deficient mouse embryos Fgf8 and Snail are both expressed, indicating that Eomes may play a role in the migration of the epiblast during gastrulation (Arnold et al, 2008).

### 1.3.2 Eomes in the mesoderm

As Eomes deficient mouse embryos arrest prior to gastrulation due to defects in the trophectoderm, the effect of Eomes knockout on gastrulation has been studied in vivo by various methods such as engineering chimaera embryos, with wildtype trophectoderm and mutant ICM (Russ et al, 2000) and engineering conditional alleles to conditionally inactivate Eomes (Arnold et al, 2008).

The role of Eomes in the development of the mesoderm was first studied in *Xenopus* and zebrafish, where it was found to activate the transcription of a plethora of mesodermal, mesendodermal and endodermal markers (Picozzi et al, 2009). Eomes was also found to be vital for normal mesendoderm development and endoderm induction (Ryan et al, 1996; Bjornson et al, 2005). Russ, et al (2000) showed the role of Eomes in murine mesoderm development by highlighting its function in the development of the mesoderm, primitive streak and the node, as well as specification of the definitive endoderm (Arnold et al, 2008).
The effect of Eomes knockout on the formation of the mesoderm was studied using chimaera knockout embryos. The embryos did not exhibit any gross abnormalities until E7.5, where the primitive streak failed to elongate and the node was absent. At E8.5, the mutant embryos resembled egg cylinders lacking mesoderm (Arnold et al, 2008) as opposed to the typical E8.5 mouse embryo in the early somite stages (Picozzi et al, 2009). Marker analysis indicates that primitive streak and mesoderm markers Bmp4, Wnt3, T and Fgf8 were expressed, albeit ectopically, in the lateral and anterior ectoderm (Arnold et al, 2008), indicating the AP axis and mesoderm is specified. Conversely, anterior mesoderm markers (Foxa2) and cardiac mesoderm marker genes (Mesp1) were not expressed in the eomes mutant embryos, indicating that while Eomes is not necessary for the specification of early mesoderm, it is crucial for the specification of these mesoderm derivatives (Arnold et al, 2008; Costello et al, 2011). In addition, the lack of expression of Eomes deficient anterior mesoderm cells in Eomes-null/wildtype chimaeras indicates that the failure to form this cell lineage is a cell autonomous function (Arnold et al, 2008). Further evidence of unaffected early mesoderm specification in Eomes deficient cells is due to the fact that Eomes deficient teratomas can form mesoderm derivatives such as muscle, cartilage and haematopoietic tissue. Furthermore, mutant cells persist in the ectoderm as opposed to migrating as per typical wildtype embryos, providing increasing evidence that Eomes plays a role in migration during gastrulation. (Arnold et al, 2008).

### 1.3.3 Eomes in the Visceral Endoderm and Axis formation.

Shortly after implantation the proximodistal axis forms in the mouse embryo as a result of interactions between the TE, epiblast and the Visceral Endoderm (VE), which eventually gives rise to the anterioposterior (AP) axis. From this point a subset of VE cells migrate distally to form the Anterior Visceral Endoderm (AVE). AP axis formation is apparent upon the induction of epiblast cells to form the primitive streak and mesoderm (Arnold et al, 2008). This study

also showed loss of Eomes to have no effect on early AP patterning. In Eomes deficient embryos the AVE forms normally with normal expression of posterior marker genes such as T and Wnt3. However, Eomes/Nodal double heterozygote mutant embryos can either arrest prior to gastrulation or suffer severe truncations of the anterior axis (Arnold et al, 2008). Furthermore, the arrested mutant embryos express the AVE and Definitive Endoderm (DE) markers Cer1 and Hex at the distal tip, indicating that the AVE is induced but fails to migrate anteriorly, in addition to abnormal proximal patterning of T, Eomes and Cripto (Arnold et al, 2008).

A second study builds on the findings that Eomes plays a crucial role in the formation of the AVE. Nodal-Smad2 was found to act upstream of eomes, activating the transcription factor in the embryonic visceral endoderm (EmVE), and conditional knockout of Eomes in the VE has no effect on the VE itself but blocks specification of the AVE. In addition Eomes was found to act upstream of Lhx1, a transcription factor known to regulate VE movement (Nowotschin et al, 2013). This is further evidence that Eomes is vital for the induction and maintenance of the AVE.

### 1.3.4 Eomes in the Definitive Endoderm

In mice, the primitive streak forms in response to TGFβ, Nodal, Wnt and Fgf signalling pathways, and gives rise to the mesoderm and definitive endoderm (DE). The DE is formed from cells within the nascent mesoderm and eventually migrates and integrates into the underlying visceral endoderm, eventually giving rise to endodermal tissues, for example the DE derived primary gut tube (Viotti, Nowotschin and Hadjantonakis, 2014; Costello et al, 2011). At E6.25 Eomes is expressed in the primitive streak of the mouse embryo. Eomes expression persists until E7.5 and is then expressed in cells within the DE which emerge from the anterior primitive streak (Arnold et al, 2008). Eomes plays a crucial role in the specification of the DE cell lineage (Arnold et al, 2008). This study utilised Eomes null ES cells to distinguish that the cells could contribute to mesoderm lineage but fail to specify into DE lineages. Furthermore, it was discovered that Eomes acts downstream of Nodal to specify DE via activation of genes vital for APS specification (Arnold et al, 2008). As previously mentioned, Eomes is vital for EMT and the migration of mesoderm cells through the primitive streak, and as a result shows Eomes to be vital for the formation and integration of the definitive endoderm (Viotti, Nowotschin and Hadjantonakis, 2014).

### 1.3.5 Eomes in Germ Cells

Eomes has been shown to play a role in the formation of human primordial germ cell like cells (hPGCLCs), an *in vitro* model of human PGCs. In order to produce hPGCLCs, human induced pluripotent stem cells (hiPSCs) first must differentiate through an incipient mesoderm like cell state (iMeLCs). During the iMeLC state WNT induces EOMES which in turn activates SOX17, a key regulator in hPGCLC specification (Kojima et al, 2017). Furthermore, Eomes has been shown to function cell autonomously prior to expression of SOX17 in hPGCLCs, indicating that Eomes may be required for germ cell competency in the primitive streak of human embryos, highlighting further divergent mechanisms of gastrulation between mammals as there are no reports that Eomes has a significant role in PGC specification of the mouse embryo (Chen et al, 2017; Mitsunaga and Shioda, 2018). This leads to the hypothesis that Eomes functions differently during gastrulation of the pig embryo, and may have a role in the specification of porcine PGCs.

### 1.3.6 Eomes in trophectoderm

Eomes is the first T-box gene to be expressed in the developing mouse embryo (Arnold et al, 2009), the first instance of which is in the trophectoderm during the early preimplantation stages, around embryonic day (E) 2.5 – 3.5. At this stage of development the trophectoderm separates from the inner cell mass (ICM) of the embryo, being driven by upregulation of Caudal-related homeobox 2 (Cdx2) or Oct3/4 respectively (Niwa et al, 2005) Eomes acts downstream of Cdx2 in trophectoderm cells (Ralston and Rossant, 2008) to promote differentiation of the trophectoderm into the extraembryonic ectoderm, containing trophoblast stem cells (TSCs) and the ectoplacental cone, the precursor to the embryonic placenta (Babiarz, Romagnano and Kurilla, 1992). The repressive effect Cdx2 exhibits upon Oct3/4 drives the trophectoderm lineage by upregulation of Eomes in the embryo. However, deletion of Cdx2 does not decrease Eomes levels in the trophectoderm and Eomes can drive trophectoderm differentiation in the absence of Cdx2, suggesting that both Eomes and Cdx2 are expressed upon Oct3/4 repression, leaving the question of how Eomes is regulated in the trophectoderm (Niwa et al, 2005). A study reported that Eomes expression in trophoblasts is autoregulated whereas Cdx2 expression is controlled by the upstream transcription factor TEAD4 (Kubaczka, Kaiser and Schorle, 2017). One study showed that Eomes deficient mouse embryos have the ability to form blastocysts but arrest at the blastocyst stage as the trophectoderm fails to differentiate. This indicates that Eomes is essential for the

development and maintenance of TSCs (Russ et al, 2000). *In vitro,* most Eomes deficient mouse embryos also do not elongate or progress past blastocyst hatching stage, but maintained this phenotype for 7 days. A small percentage of these embryos showed late spreading of trophoblast like cells before degenerating (Russ et al, 2000). These findings contrast with the blastocyst development of the pig. A study previously carried out in our laboratory found extraembryonic EOMES to be present only in the late elongation stage of porcine blastocyst development, indicating that there are fundamental differences in the mechanisms of trophectoderm differentiation between mice and pigs (Magaña et al, 2014).

## 1.4. The Sry-Box protein family in early development

The Sry-Box (Sox) family of proteins play a crucial role in embryogenesis, during which they act as transcription factors and have the ability to bind to and modify DNA. The Sox proteins are characterised by a 79 amino acid motif named the Sry-box. This Motif encodes a specialised high mobility group (HMG) DNA binding domain, which is highly conserved across vertebrates (Hou, Srivastava and Jauch, 2017; Penvey and Lovell-Badge, 1997). The 20 Sox proteins found in mammals can be divided into 7 groups dependant on the sequence homology of the DNA binding domain between the respective proteins (Wegner, 2010).

Sox17 is a member of the SoxF group, alongside Sox7 and Sox18, which share a group due to the structure containing two separate transactivation domains. (Wegner, 2010). The first function of Sox17 was discovered in 1996, where it was found to activate transcription during mouse spermatogenesis (Kanai et al, 1996). Since this discovery Sox17 has been found to carry out a role in lineage segregation, during gastrulation in Xenopus, Zebrafish and Mouse, ultimately determining endoderm specification. (Kanai-Azuma et al, 2002; Hudson et al, 1997; Alexander and Stainer, 1999). In addition, Sox17 has also been shown to be a key regulator of PGC fate (Irie et al, 2015), and also plays a role in maintaining the integrity of the primitive endoderm of mouse embryos and potentially facilitates its differentiation into primitive endoderm (Artus, Piliszek and Hadjantonakis, 2011)

### 1.4.1 Sox17 in the definitive endoderm

In the mouse embryo Sox17 mRNA is first detected in the visceral endoderm, pre streak (E6-6.25), and the expression spreads to the rest of the extraembryonic visceral endoderm by early streak (E6.5). Sox17 is not expressed in the embryonic tissues until mid-streak (E7.0),

where expression arises in the endoderm, below the anterior primitive streak, the point at which the definitive endoderm is specified (Kanai-Azuma et al, 2002, Martinez Barbera et al, 2000). At E7.5 Sox17 expression further extends to the endoderm below the neural plate and at E7.75 Sox17 expression is present in the prospective foregut endoderm, but expression is reduced in both the foregut and definitive endoderm by E8.0. By E8.25, or the three to five somite stage, Sox17 expression resides in the posterior endoderm and by the seven to eight somite stage expression is mainly localised in the midgut and hindgut of the embryo. Sox17 expression disappears from the posterior gut endoderm at E9.0 (Kanai-Azuma et al, 2002).

The role of Sox17 in the mouse embryo has been studied by creating Sox17-null embryos and examining the phenotype throughout early gestation. Overall, loss of Sox17 impairs the expansion of the endoderm into the midgut and hindgut, while facilitating apoptosis on cells within the foregut endoderm. There are a lack of defects in the visceral endoderm, suggesting that Sox17 does not play a major role in the specification or maintenance of this tissue, or that the co-expressed Sox7 rescues the cells and allows them to form visceral endoderm. Despite Sox17 being expressed at E7.0 in the embryo proper, gross morphological changes were not observable in the null embryo until E8.5, where the embryos lacked axis rotation and suffered from stunted growth, but otherwise maintained relatively normal structure considering that the definitive endoderm is required for the morphogenesis of some mesoderm and ectoderm derived tissues in vertebrates. This may be explained by the presence of several genes in the gut endoderm, for example Hex, Cer1 and Cdx2, which can exert this morphogenetic activity prior to the apoptotic events at E8.0 (Kanai-Azuma et al, 2002; Martinez Barbera et al, 2000; Withington, Beddington and Cooke, 2001; Chi et al, 2011, van de Ven et al, 2011).

There is evidence that Sox17 carries out differential roles within the endoderm. Increased apoptosis in the foregut of Sox17-null embryos suggests that Sox17 acts as a maintenance factor whereas the abolishment of differentiation in the rest of the gut suggests that Sox17 also plays a role in the differentiation of the endoderm (Kanai-Azuma et al, 2002). The Sox17 null phenotype then gives rise to aberrant primordia tissues, causing loss of gallbladder and bile duct progenitors (Uemura et al, 2010).

### 1.4.2 Sox17 in PGCs

Primordial Germ Cells (PGCs) are the precursor cells which eventually give rise to spermatozoa or oocytes, and are the cells responsible for generating totipotency. (Saitou, Barton and

Surani, 2002). Mammalian PGCs was first established in the mouse model, where competency for the germ cell lineage was found to be established in the proximal epiblast of the mouse embryo at E6.25 (Hayashi, de Sousa Lopes and Surani, 2007). The PGC lineage in mouse is established from a small number of founder PGCs in an area responsive to Bmp signalling and are completely abolished in Bmp4 null embryos (Lawson et al, 1999). This area of the proximal epiblast also gives rise to extraembryonic mesoderm and the allantois. (Saitou, Barton and Surani, 2002; Lawson et al, 1999). These founder cells were recruited from a population of cells which express *fragilis*, a transmembrane protein that promotes germ cell competence. This community of cells was discovered to be destined for mesoderm fate, as they have high expression of Fgf8 and Brachyury, however, expression of *stella* facilitates downregulation of homeobox genes within these cells allowing the escape of this fate and ultimately enabling the cells to reacquire pluripotency. (Saitou, Barton and Surani, 2002).

In the mouse embryo, PGC migration propagates at approximately E6.25, proceeding to migrate to the extraembryonic mesoderm and then the hindgut endoderm at E7.25 and E7.5 respectively. The PGCs then collect in the genital ridges at E9.5-10.5 (Artus, Piliszek and Hadjantonakis, 2011). Sox-17 null embryos exhibited no difference in PGC specification and colonisation in the allantois in comparison to wildtype controls at early headfold stage (E7.5). However, later migration patterns become aberrant as lateral movement in gut endoderm is abolished, causing lack of PGCs in the gut. The PGCs instead collected in the extraembryonic endoderm. Chimaera studies show that PGC migration is rescued upon expression of wildtype endoderm in the Sox17 null embryo (Artus, Piliszek and Hadjantonakis, 2011). This can be explained by the defective endoderm as previously discussed, causing PGCs to be trapped within the hindgut, and exacerbated by expression of the adhesion protein e-cadherin, which is known to affect endoderm morphology in the mouse embryo, within the gut endoderm of Sox17 null embryos. (Burtscher and Lickert, 2009; Artus, Piliszek and Hadjantonakis, 2011). These findings show that Sox17 is vital for PCG migration in the mouse embryo as an indirect effect of maintaining the structure of the endoderm, enabling PGCs to migrate normally.

A study utilising human PGC-like cells (hPGCLCs), an *in vitro* model of human PGCs created by differentiation of human embryonic stem cells (hESCs), demonstrates that Sox17 plays differing roles in these cells and mouse PGCs (Irie et al, 2015). Dissimilar to its indirect role in mouse PGCs, Sox17 was shown to be the key regulator of specification in hPGCLCs. Sox17 is sparsely expressed alongside the mesoderm gene T in day 1 embryoid bodies, which are

defined as spontaneously differentiated ESCs that form 3 dimensional clusters of cells representing the germ layers (Kurosawa, 2007). Sox17 expression in these embryoids leads to the autonomous induction of known germ cell genes namely Blimp1, Nanos3 and Tfap2c, key regulators of human PGCs (Sugawa et al, 2015; Julaton and Reijo Pera, 2011; Mitsunaga et al, 2017). In addition, Sox17 null cells fail to undergo PGC specification, and loss of Sox17 in Tcam-2 seminoma, a cell line derived from germ cell tumours, causes downregulation of germ cell specific genes, indicating that Sox17 acts upstream of critical PCG regulatory genes and may play an important role in human PGC maintenance (Saitou, Barton and Surani, 2002).

In the porcine embryo PGCs originate from the epiblast prior to primitive streak formation. BMP and WNT signalling causes upregulation of SOX17 and BLIMP1. SOX17 is necessary for both PGC and definitive endoderm regulation, and coexpression of BLIMP1 represses the SOX17 endoderm genes, leading to PGC fate. Additionally, SOX17 and BLIMP1 coexpression initiates the germline specific epigenetic programme (Kobayashi et al, 2017), a reset of the full germline potency and erases epigenetic mutations, genomic imprints and poises the germline for transfer of genetic information upon fertilisation (Tang et al, 2015). Deletion of SOX17 in the mouse embryo causes no changes in PGC morphology, but migration is affected due to aberrant endoderm (Saitou, Barton and Surani, 2002). This highlights a difference between murine and porcine PGC development as SOX17 appears to play a more crucial role in pigs. These differences could be further expanded on by SOX17 knockout studies in pigs.

## 1.5 Hypothesis and aims

The following hypotheses are based on the current literature and preliminary data gathered from previous experiments within our lab. The first hypothesis is that IL-6 plays a role in maintenance of pluripotency in the pig embryo, potentially filling in the role that LIF plays in the mouse embryo. The second hypothesis states that the role of Eomes in the gastrulating embryo, in particular formation of the mesendoderm, is not conserved between pigs and mice. The aim of this study is to understand the role of IL-6 and Eomes in the preimplantation pig embryo by studying the effect of IL-6 inhibition and gene knockouts mediated by CRISPR-Cas9.

To elucidate the role of IL-6 in the porcine embryo, embryos will be cultured in the presence of IL-6 and a novel small molecule IL-6 inhibitor. The total cell numbers will be assessed by staining, along with the amount of ICM and TE to understand if IL-6 has any effect on either of the lineages of the blastocyst. Furthermore, the pluripotent state of the embryo will be

assessed by visualising the proportion of Nanog and SOX17 expressing cells in the ICM, to understand if IL-6 plays a role in maintaining the pluripotent state of the embryo. These experiments will be first conducted *in vitro*, using parthenogenetically activated pig embryos as a model for early embryogenesis. This experiment will be repeated with embryos collected from artificially inseminated sows to gain a clearer insight into the role IL-6 plays *in vivo*. CRISPR-Cas9 genome editing techniques will also be applied to *in vitro* parthenotes to create IL-6 knockout embryos to assess any aberrant phenotypes that knockout of IL-6 may cause. If a successful and repeatable genome editing protocol is created this experiment will be repeated with *in vivo* embryos.

In order to understand the role of Eomes in during gastrulation in the porcine embryo, an efficient method for creating Eomes knockout embryos must first be developed. This is due to Eomes expression in the porcine embryo being first apparent at E11, meaning *in vitro* studies are not applicable. Due to the small amount of embryos that can be studied in a single *in vivo* study the gene editing technique must be optimised to ensure a high editing efficiency and to minimise embryo death after the intensive microinjection procedure necessary for creating knockout embryos. To optimise the gene editing procedure I will first design multiple guide RNAs and test the editing efficiency of the guides in parthenote embryos. Adjustments will be made to the methodology in order to increase the editing efficiency with consecutive experimental runs. When an acceptable editing efficiency has been reached embryos will be collected from sows at the one cell stage and microinjected with Cas9-gRNA to knock out Eomes. These Embryos will be transferred into surrogate sows and collected at E11, early somites stage and late somites stage, in order to assess any phenotypic abnormalities across the 3 developmental stages and to gain a wider insight into the role Eomes plays at this stage.

# 2. Materials and methods:

## Ethical considerations:

All laboratory work carried out during this project falls under ethical approval gained by Dr Ramiro Alberio, for work under his supervision.

## 2.1 Oocyte/Embryo collection:

Porcine ovaries were transported from a nearby slaughterhouse to the laboratory immediately after slaughter. Ovaries were immediately washed with ethanol and warm PBS, and then held in PBS at 39°C until aspiration. Oocytes were extracted from the ovaries with a 30g x 0.5" hypodermic needle, 10mL syringe and allowed to sediment in a 50mL falcon tube at 39°C. The sediment was collected placed in an in house TCM-199 (+HEPES) based medium for searching (Table 1).

High quality cumulus oocyte complexes (COCs) were collected and washed in a separate dish of search medium before being washed in a well of TCM-199 based *in vitro* maturation medium (IVM; Table 2). 50-60 COCs were placed per well of IVM and incubated for 44 hours, 37.5°C, 5% $CO_2$.

All media was allowed to equilibrate for at least 2 hours prior to use, in their final incubating conditions. Media was prepared the day before ovaries arrived, with the growth factors and hormones being added to the IVM just prior to equilibration on the day of aspiration. PBS, petri dishes and collection tubs all warmed to 39°C in the morning prior to aspiration.

For embryos collected for *ex vivo* culture, the uterine tracts were collected from pregnant sows and flushed with warm PBS, 1% FCS. The PBS was searched and embryos were placed directly into PZM5 medium for culture.

*Table 1 - Search medium recipe*

| Search component | Volume added | Catalogue number |
|---|---|---|
| TCM-199 (+HEPES) | 20 mL | Sigma, M7528 |
| BSA | 40 mg | Fisher, BP9705 |
| L-Glutamine | 2 mg | Sigma, G8540 |
| Penicillin/Streptomycin | 100 µL | Sigma, P4333 |
| pH: 7.3 – 7.4 (adjust with HCl/NaOH accordingly)<br>mOsmo: 290 – 300<br>Filter and use within one week | | |

*Table 2 - In vitro maturation medium recipe*

| IVM component | Volume added | Stock concentration (mg/mL) | Catalogue number |
|---|---|---|---|
| TCM-199 (-HEPES) | 10 mL | | Sigma, M2154 |
| L-Glutamine | 1 mg | | Sigma, G8540 |
| Glucose | 5.496 mg | | Sigma, g7021 |
| PVA | 10 mg | | Sigma, p8136 |
| Cystiene | 10 µL stock | 69 | Sigma, c7352 |
| Sodium Pyruvate | 8.33 µL stock | 120 | Sigma, p4562 |
| FSH | 0.108 µL stock | 0.924 | Sigma, f2293 |
| LH | 4.4 µL stock | 1.13 | Sigma, l5269 |
| EGF | 1 µL stock | 100 | Sigma, s4127 |
| FGF | 1 µL stock | 80 | Made in house |
| IGF | 5 µL stock | 200 | Peprotech, CYT-022 |
| LIF | 1 µL stock | 200 | Millipore, LIF1050 |
| Penicillin/Streptomycin | 50 µL stock | | Sigma, P4333 |
| pH: 7.3 – 7.4 (adjust with HCl/NaOH accordingly)<br>mOsmo: 290 – 300<br>Filter and use within one week | | | |

## 2.2 Parthenogenetic activation and blastocyst generation:

After 44h maturation the oocytes were denuded with 1mg/mL hyaluronidase (Sigma, H3506) in order to remove cumulus cells. Oocytes were searched and the mature oocytes with apparent polar bodies were separated and held in search media for later use. Prior to activation the oocytes were equilibrated in activation media. The oocytes were placed in activation media in an Eppendorf micro fusion chamber and allowed to settle between the electrodes (0.5 mm). The oocytes were activated using an Eppendorf multiporator (110 V, 30 µs, 2 pulses) and placed into PZM5 fertilisation media supplemented with 2mM 6-Dimethylaminopurine (DMAP; Sigma, D2629) and 5 µg/ ml Cytochalasin B (Acros Organics, 228090010) for 5 hours before being placed into porcine zygote medium (PZM5) for 5 days. On the morning of day 5 morulae and blastocysts were selected and placed into equilibrated N2B27 media to promote blastocyst growth and hatching.

*Table 3 - Porcine zygote medium recipe*

| PZM5 stock component | Volume added | Stock concentration | Catalogue number |
|---|---|---|---|
| Water | 100 mL | | |
| NaCl | 630 mg | 108 mM | Sigma, S5886 |
| KCl | 74.6 mg | 10 mM | Sigma, P5405 |
| KH2PO4 | 4.8 mg | 0.35 mM | Sigma, P5655 |
| MgSO4 | 4.8 mg | 0.40 mM | Sigma, M2643 |
| NaHCO3 | 210.6 mg | 25.07 mM | Sigma, S5761 |
| L-glutamine | 29.2 mg | 2.0 mM | Sigma, G8540 |
| Na pyruvate | 2.2 mg | 0.2 mM | Sigma, P4562 |
| Calcium lactate | 43.6 mg | 2.0 mM | Sigma, C8356 |
| pH: 7.3 – 7.4 (adjust with HCl/NaOH accordingly)<br>mOsmo: 278 – 298 mOsm, Filter and use within 1 month | | | |
| PZM5 working media component | Volume added | Concentration | Catalogue number |
| PZM5 stock | 10 mL | | |
| Hypotaurine | 100 µL | 55 mg/mL | Sigma, H1384 |
| BSA | 40 mg | 4 mg/ml | Fisher, BP9705 |
| BME | 200 µL | | Sigma, B6766 |
| MEM | 100 µL | | Sigma, M7415 |
| Gentamycin | 10 µL | 50 mg/ml | Sigma, G1914 |
| Filter and use within 1 week | | | |

*Table 4 - Activation medium recipe*

| Activation media component | Volume added | Concentration | Catalogue number |
|---|---|---|---|
| Water | 100 ml | | |
| PVA | 100 mg | 1 mg/ml | Sigma P8136 |
| D-Mannitol | 5.1 g | 280 mM | Sigma M4125 |
| Cacl2.H20 | 58.8 µl | 0.1 mM | Sigma C7902 |
| MgSO4.7H20 | 84 µL | 0.1 mM | Sigma M1880 |

*Table 5 - N2B27 medium recipe*

| N2B27 media component | Volume added | Catalogue number |
|---|---|---|
| DMEM/F12 medium | 23.5 ml | Gibco, 11320-074 |
| Neurobasal Medium | 23.5 ml | Gibco, 21103-049 |
| N2 supplement | 0.5 ml | Gibco, 17502-048 |
| B27 supplement | 1 ml | Gibco, 17504-046 |
| L-glutamine | 0.5 ml | Sigma, G8540 |
| Penicillin/streptomycin | 0.5 ml | Sigma, P4333 |
| Fatty acid free BSA | 0.15 g | Sigma, A8806 |

## 2.3 Guide RNA synthesis and preparation:

2 batches of gRNAs were prepared during this study, one prepared via a cloning/bacterial transfection method, and one was prepared with a cloning free gRNA synthesis kit.

The cloning method was conducted as stated by Talbot and Amacher, 2014, using a DR274 plasmid based method. Bacterial transformation was carried out as stated by Lamitina, 2007. gRNA synthesis and cleanup was conducted with Maxiscript T7 kit (Thermo, AM1312). This was carried using RNAse free technique.

Cloning free method was carried out with GeneArt™ Precision gRNA Synthesis Kit (Invitrogen, A29377). This was carried using RNAse free technique.

Guide RNA-Cas9 Ribonucleoprotein mix was prepared 30 minutes prior to injection. 1 µl of each guide was mixed with 1 µl of Cas9 and incubated for 20 minutes at 37°C. 1 µl of each guide mix was added to TE buffer to a total of 10 µl. This was carried using RNAse free technique.

## 2.4 Porcine oocyte microinjection

Porcine oocytes microinjections were performed at 44-48 hours post maturation. During microinjection the oocytes were held in search media supplemented with 5µg/ml cytochalacin B, submerged in mineral oil on a 39°C heated stage. Oocytes were stabilised with a holding pipette (Hunter Scientific, 2021.9), and microinjected with gRNA and Cas9 ribonucleoprotein complex backfilled microinjection needles (Origio, Mic-35-30-BIO). The oocytes were parthenogenetically activated and cultured in PZM5 fertilisation medium supplemented with (2 mM DMAP and 5µg/ml cytochalasin b).

## 2.5 DNA extraction and genotyping

Blastocysts were collected from day 6 onwards. Zona pellucida removal was carried out by briefly submerging blastocysts in acid Tyrodes solution (Sigma, T1788) and washed in PBS supplemented with 1% BSA. The blastocysts were placed in 2.5 µl accutase and 5 µl lysis buffer (50 mM NaOH, 0.4 mM EDTA). The blastocysts were heated at 99°C for 20 minutes in a thermocycler, neutralised in 5 µl Tris-HCl (40 mM) and stored at -20°C.

Nested PCR analysis was carried out to originally amplify a fragment flanking the target sequence, with a second PCR to target a smaller amplicon. Primers were designed to flank the CRISPR target sequence (Eurofins). DMSO was added to Eomes master mixes to prevent the GC rich primers dimerising. Second PCRs run in 20 µl reactions to run on acrylamide and PAGE gels.

*Table 6 - List of primers used for genes studied*

| Gene | Accession number | Forward primer | Reverse primer | Target length | Annealing temperature |
|---|---|---|---|---|---|
| Eomes g1 (F1R1) | NC_010455.5 | CCAAGAAGTTTT CGGGCAGC | CGGGGGACTG GAGGTAGTAG | 291 bp | 62 |
| Eomes g2 + g3 (F2R2) | NC_010455.5 | GCTCGCTCTTCC CGTACC | GCTCGCTCTTC CCGTACC | 455 bp | 62 |
| IL6 | NC_010451.4 | TGCTTCTGGTGA TGGCTACT | TCCAGCCCCGC AGTATATTT | 387 bp | 60 |

First Eomes PCR (all guides)

*Table 7 - F1R2 PCR mix (Eomes)*

| Master mix component | Volume (per sample) | Catalogue number |
|---|---|---|
| KAPA mix | 5 µl | KAPA biosystems KK1006 |
| F1 primer | 0.1 µl | |
| R2 Primer | 0.1 µl | |
| DMSO | 0.25 µl | |
| $H_20$ | 3.55 µl | PCRH20-RO |
| Genomic DNA | 1 µl | |

*Table 8 - F1R1 PCR Mix (Eomes Guide 1)*

| Master mix component | Volume (per sample) | Catalogue number |
|---|---|---|
| Sigma mix | 10 µl | Sigma P4600 |
| F1 primer | 0.5 µl | |
| R1 Primer | 0.5 µl | |
| DMSO | 0.2 µl | |
| $H_20$ | 6.8 µl | PCRH20-RO |
| 1:10 DNA (first PCR product) | 2 µl | |

*Table 9 - F2R2 PCR mix (Eomes Guide 2+3)*

| Master mix component | Volume (per sample) | Catalogue number |
|---|---|---|
| Sigma mix | 10 µl | Sigma P4600 |
| F2 primer | 0.5 µl | |
| R2 Primer | 0.5 µl | |
| DMSO | 0.2 µl | |
| $H_20$ | 6.8 µl | PCRH20-RO |
| 1:10 DNA (first PCR product) | 2 µl | |

*Table 10 - First PCR mix for IL6 fragment with proofreading KAPA polymerase*

| Master mix component | Volume (per sample) | Catalogue number |
|---|---|---|
| KAPA mix | 5 µl | KAPA biosystems KK1006 |
| F primer | 0.1 µl | |
| R Primer | 0.1 µl | |
| $H_20$ | 3.8 µl | PCRH20-RO |
| Genomic DNA | 1 µl | |

*Table 11 - Second PCR for IL6 fragment*

| Master mix component | Volume (per sample) | Catalogue number |
|---|---|---|
| Sigma mix | 10 µl | Sigma P4600 |
| F2 primer | 0.5 µl | |
| R2 Primer | 0.5 µl | |
| $H_20$ | 7 µl | PCRH20-RO |
| 1:10 DNA (first PCR product) | 2 µl | |

PCR products were run on 1.5% agarose gels made up in TAE buffer for approximately 40 minutes, 100 V. DNA was extracted from gel slices using a Machery-Nagel PCR clean up gel extraction kit (740609). DNA concentration was measured on a nanodrop and adjusted to 10ng/µl prior to being sent for sequencing.

Multiplex DNA analysis was carried out to visualise any editing events on a gel. The samples were reannealed (95$^{o}$C 5mins; 85$^{o}$C 5 secs; 25$^{o}$C 5 secs) and run on a polyacrylamide gel. The gels were prepared in house and left to stand for an hour after preparation. The gels were run at 190 V for 2.5 hours. After electrophoresis the polyacrylamide gel was submerged in ethidium bromide solution and placed on a rocker in a dark box for 15 minutes. All gels were visualised and imaged on a UVP GelDoc-It imaging system (analytikjena, 97-0578-01).

*Table 12 - Polyacrylamide gel recipe*

| Component | Volume added | Catalogue number |
|---|---|---|
| Water | 1.74 ml | |
| 5x TBE buffer | 1.2 ml | |
| 30% acrylamide mix | 3 ml | Flowgen, H17009 |
| TEMED | 3 µl | Fisher, BP150-100 |
| 10% ammonium persulphate | 75 µl | Sigma, A3678 |

## 2.6 Immunofluorescence staining of blastocysts

Blastocysts were collected from day 6 onwards and zona pellucida was removed with acid Tyrodes solution (Sigma, T1788). Blastocysts were washed briefly in PBS supplemented with 1% BSA and fixed in 2% PFA for 15 minutes. After fixation the blastocysts were placed in 125 mM glycine for 5 minutes to quench excess PFA, and then placed in PBS supplemented with 1% BSA and stored at 4°C to be stained.

On the day of primary staining fixed blastocysts were placed in permeabilisation solution (PBS supplemented with 0.2% Triton x-100) for 15 minutes prior to being placed in blocking solution (PBS supplemented with 10% donkey serum and 0.1% tween-20) for an hour and incubated at room temperature. The blastocysts were placed in primary antibodies diluted with blocking solution and incubated at 4°C overnight.

The blastocysts were washed in four 15 minute increments in washing solution (PBS supplemented with 1% BSA and 0.1% Tween 20). Blastocysts were stained with secondary antibodies diluted in blocking solution for one hour at room temperature, shielded from light. The blastocysts were washed again as before and mounted on 5 well slides (Thermo, ER-307W-CE24) with Fluoroshield with DAPI (Sigma, F6182). The blastocysts were analysed with a Leica DM400B fluorescent microscope. Stained cells were counted using ImageJ software.

*Post staining genotype analysis:*

Method as above until mounting. The blastocysts were added to 1:200 Hoechst solution for nuclear staining and mounted to slides in PBS. After analysis the coverslips were carefully removes and blastocysts aspirated and placed in 2.5 µl accutase and 5 µl lysis buffer (50 mM NaOH, 0.4 mM EDTA). The blastocysts were heated at 99°C for 20 minutes in a thermocycler, neutralised in 5 µl Tris-HCl (40 mM) and stored at -20°C. Genotype analysis was carried out as per section 2.5.

*Table 13 - Antibodies used and dilutions*

| Antibody | Species | Dilution | Catalogue number |
|---|---|---|---|
| Nanog | Rabbit | 1:500 | Peprotech, 500-P236 |
| Sox17 | Goat | 1:300 | R+D, AF1924 |
| Sox2 | Goat | 1:500 | Santa-Cruz, sc-17320 |
| Anti goat Cy3 | Donkey | 1:500 | Jackson, 705-165-003 |
| Anti rabbit Alexa 488 | Donkey | 1:500 | Invitrogen, A-21206 |

## 2.7 Embryo treatments and inhibition:

Embryos were matured, activated and left to develop until late day 4. Morulae were selected and added to treated N2B27 medium and allowed to develop into blastocysts. Blastocysts were collected from day 6 onwards and stained as per section 2.6. As LMT-28 was dissolved in DMSO, a proportional amount of DMSO was added to all other wells (1:1000) as a control measure.

*Table 14 - Embryo treatments and concentrations*

| Treatment | Concentration | Catalogue number |
|---|---|---|
| LMT-28 | 30 mM | Sigma, SML1628 |
| LIF | 1 ng/ml | Peprotech, 300-05 |
| IL6 | 10 ng/ml | Novus, 686-PI-025 |
| TGFB | 10 ng/ml | Peprotech, 100-21 |

### Experimental design of IL-6 inhibition experiments.

Embryos were collected *ex vivo* or matured and activated *in vitro* as described above. In both sets of experiments the E5 morulae were treated with LMT-28 to inhibit IL-6 signalling, IL-6 and TGFB. LIF treatment was excluded from the ex vivo morulae due to small sample size.

Treated embryos were stained for SOX17 and NANOG to assess lineage segregation into hypoblast and ICM during blastulation in the different treatments. Cell number and staining was analysed with ImageJ software.

*In vitro* blastocysts analysed: LMT-28 treated (n) = 16, LIF treated (n) = 10, IL-6 treated (n) = 14, TGFB treated (n) = 9, Control (n) = 5. Results compiled from 2 repeats.

*Ex vivo* blastocysts analysed: LMT-28 treated (n) = 13, IL-6 treated (n) = 8, TGFB treated (n) = 9, Control (n) = 5. Results compiled from one experiment.

# 3. Interleukin-6 Results

## 3.1 IL-6 family expression in the preimplantation embryo:

It has been long established that IL-6 is present in the early mouse embryo (Lee, 1992). In addition, LIF, a known member of the IL-6 cytokine family plays a role in maintaining pluripotency in mouse embryonic stem cells (mESCs) by activating the STAT3 signalling pathway. LIF activation is mediated via GP130, or IL-6 signal transducer (IL6ST), a receptor subunit shared between members if the IL-6 cytokine family (Matsuda et al, 1999). Our scRNAseq data of preimplantation porcine embryos showed no expression of LIF, and very low levels of LIF receptor (LIFR). IL-6 was highly expressed in the E5 morula and E6 TE whereas IL-6 receptor (IL6R) was expressed mainly in the E6 ICM, indicating a possible paracrine signalling mechanism between the TE and ICM. IL6ST was expressed in all measured stages and tissues of the early pig embryo (Figure 4).

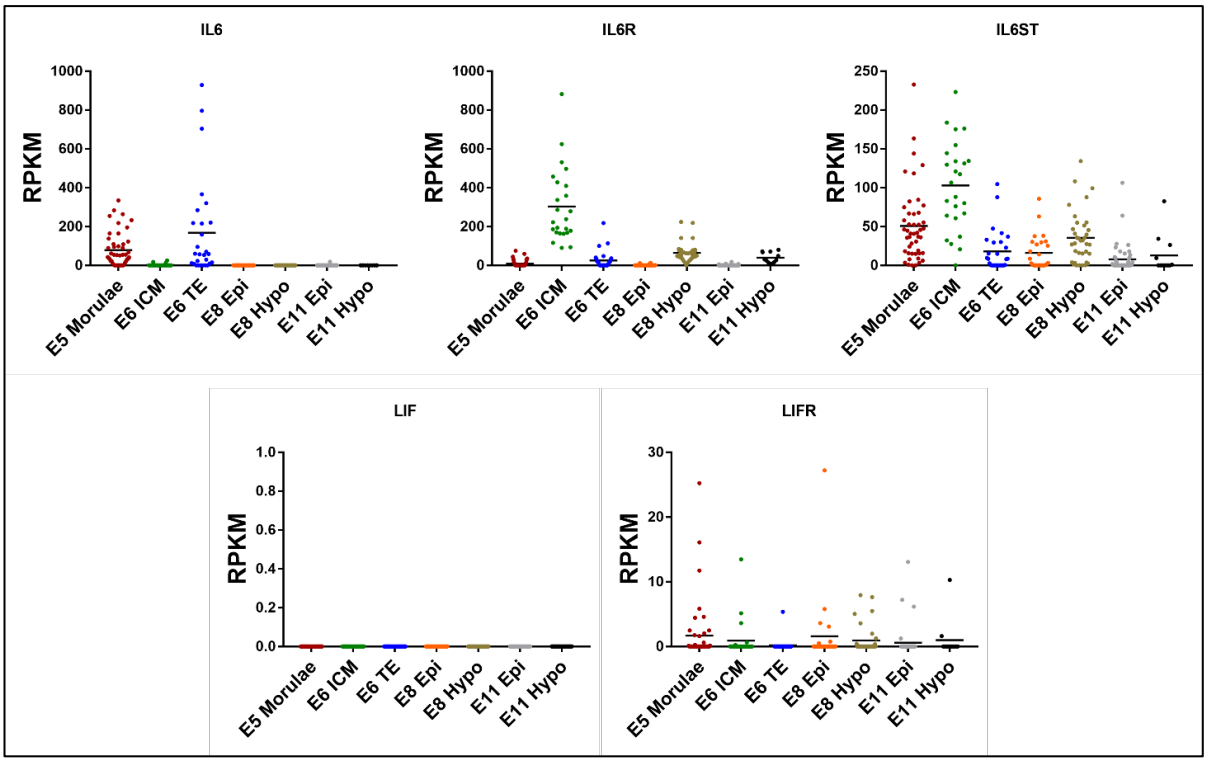



*Figure 4 - Dot plots of the expression of key members and receptors of the IL-6 cytokine family in differing stages of the pre-primitive streak porcine embryo, with each point representing one cell from the corresponding embryonic stage. RPKM - Reads per kilobase of transcript per million mapped reads.*

In order to assess the role IL-6 plays on the developing porcine embryo, late E4-early E5 morulae were treated with IL-6, LIF and a novel IL-6 inhibitor, LMT-28.

## 3.2 IL-6 Supplementation and inhibition on *in vitro* embryos

Electrically activated parthenogenetic embryos were cultured until morula stage and treated with LMT-28, IL-6 and LIF. An untreated group was run in parallel as a control. In order to assess changes within the embryo the late E6 blastocysts were collected and stained for SOX17 and NANOG, to assess number of ICM cells and hypoblast segregation (Ramos-Ibeas et al, 2018). Prior to fixation the blastocysts were imaged to assess any gross morphological changes as a result of the treatments (Figure 5).

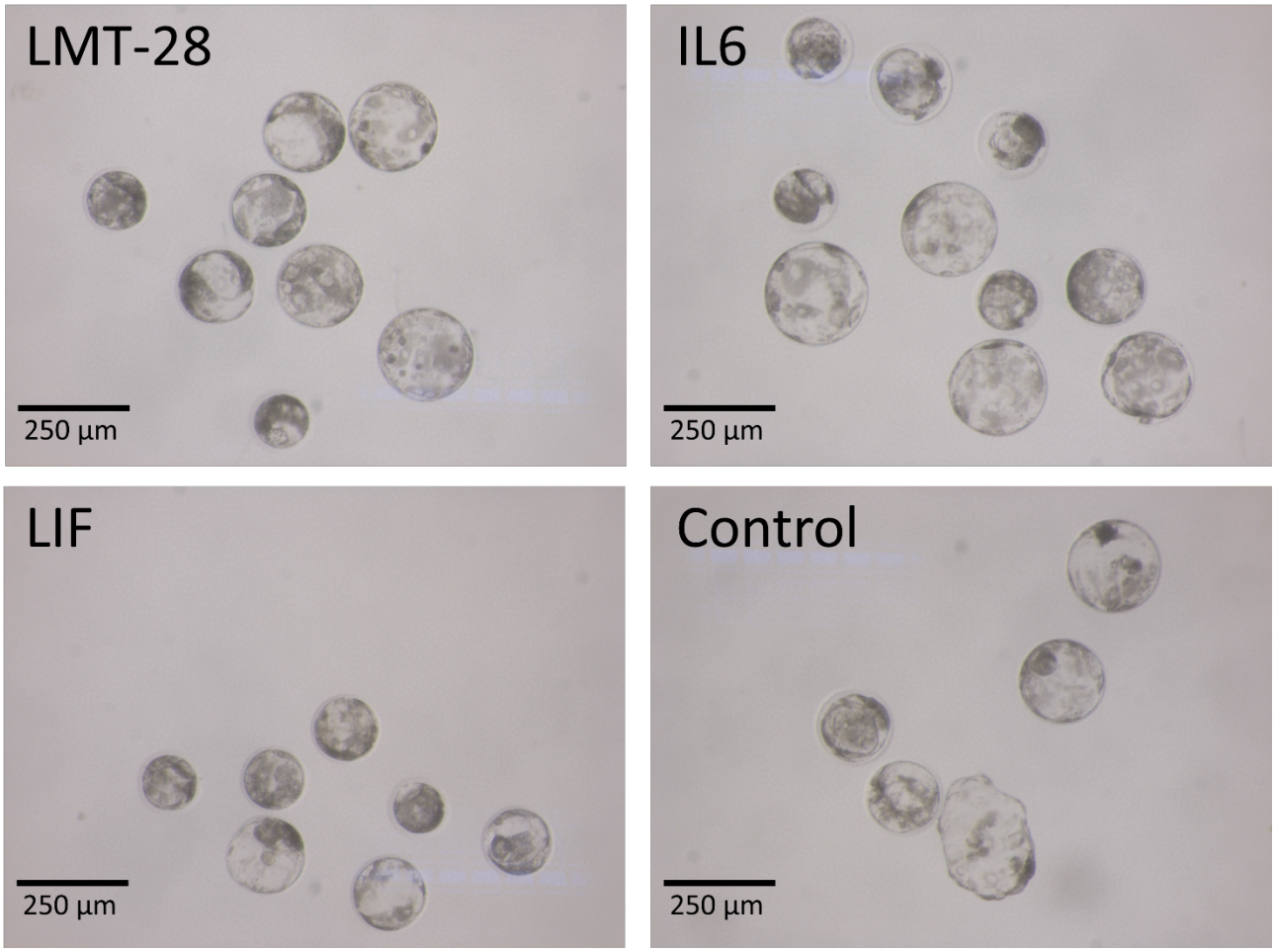



*Figure 5 - Brightfield images of treated pig blastocysts at late E6. Expanded LMT-28 treated embryos were slightly reduced in size in comparison to the controls, whereas the IL-6 treatment group had an increase in size of expanded blastocysts.*

The LIF group displayed the most drastic morphological difference from the controls, as expansion was poor and growth was stunted. 42% of blastocysts in the LIF group expanded, compared to 75% in the LMT-28 group, 50% in the IL-6 group and 60% in the control group.

The control group possessed a single hatched embryo. No hatching occurred in the other groups.

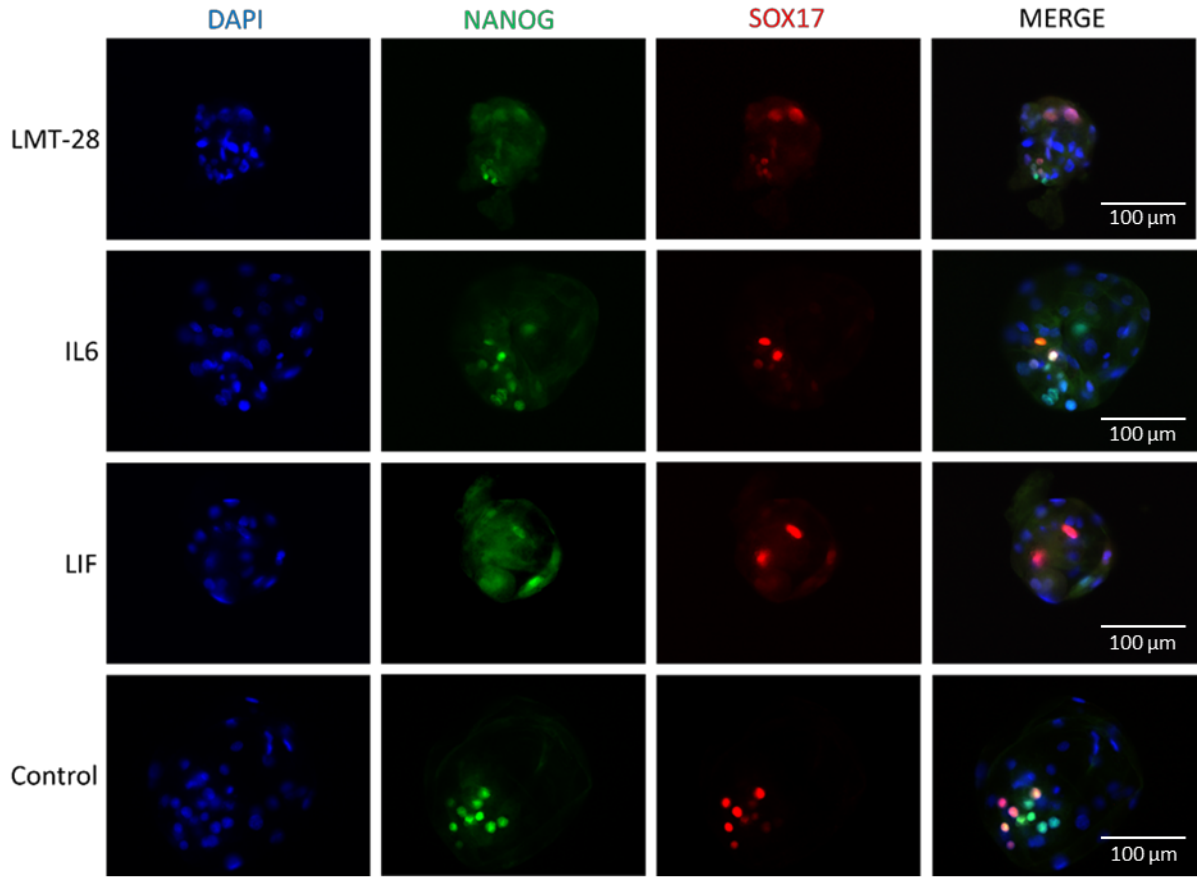



*Figure 6 – Representative immunofluorescence staining images from each of the treatment groups.*

SOX17 and NANOG were detected in all groups, and depict the location of the ICM within the embryo. Total cell number was deduced by the number of DAPI positive cells present in each embryo (Figure 6). Total cell number, TE cells and ICM cells were counted in every embryo stained to establish if IL-6 had an effect on the growth of the 2 (TE, ICM) distinct populations of the blastocyst (Figure 7).

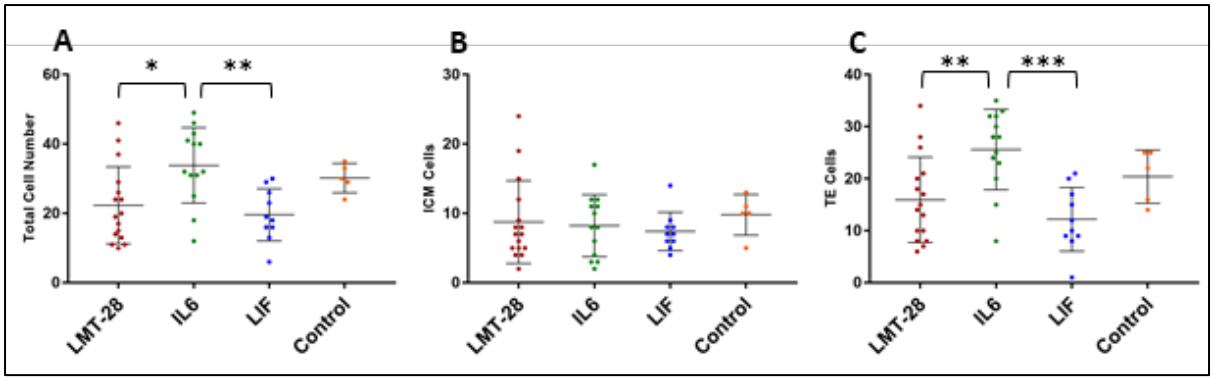



*Figure 7 - Number of cells in the treated parthenote embryos. A) Total cell number of the embryos deduced by all DAPI stained cells. B) ICM population of the embryos deduced by all SOX17 or NANOG positive cells. Costained cells were only counted once. C) TE cell population deduced by subtracting ICM cell number from total cell number. Each point represents one embryo.*

A) 1 way ANOVA (P = 0.0038). Tukey's multiple comparison test showed significant difference between LMT-28 and IL-6 (P = 0.0157), and IL-6 and LIF (P = 0.0069).
B) Kruskal-Wallis test (ICM data not normally distributed) determined no significant difference between all groups.
C) 1 way ANOVA (P = 0.0005). Tukey's multiple comparison test showed significant difference between LMT-28 and IL-6 (P = 0.0058), and IL-6 and LIF (P = 0.0005).

Another means of assessing not only the quality of embryos but also the effect of the treatments on the embryos was to measure the ICM:TE ratio as seen in figure 5. Typically, ICM:TE of *in vivo* porcine embryos is approximately 0.3, with *in vitro* embryos having a higher TE count (Koo et al, 2004). The LIF group had an increased ICM:TE ratio compared to the other groups, suggesting impairment of the trophectoderm lineage (Figure 8).

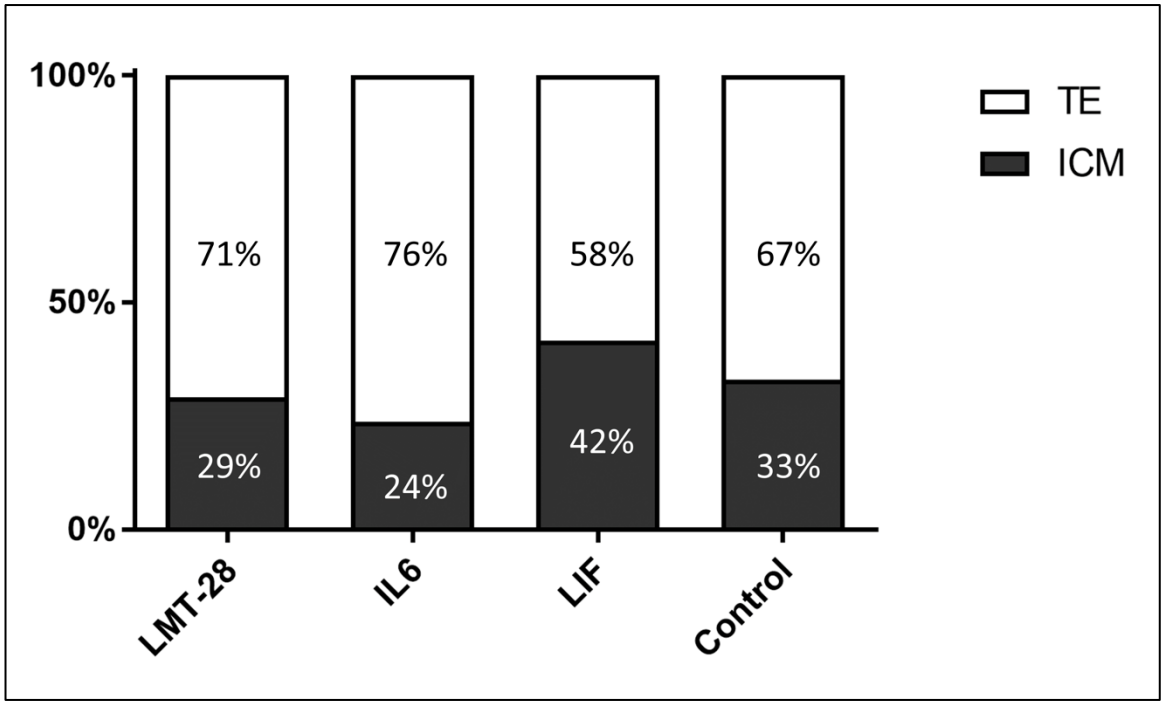



*Figure 8 – ICM:TE ratio percentage mean of the 4 blastocyst groups. The ratio was calculated by dividing NANOG and SOX17 positive cells (ICM) by the number of cells stained with DAPI only (TE).*

In order to assess if IL-6 plays a role in the maintenance of pluripotency in the ICM, the amount of NANOG and SOX17 positive cells were quantified in each embryo and plotted on a scatter plot (Figure 9).

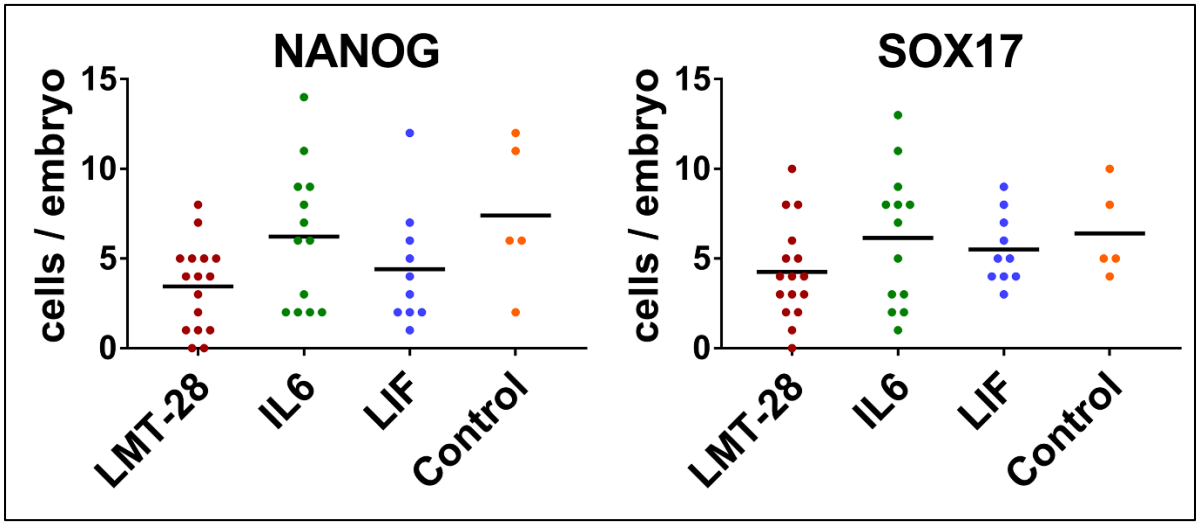



*Figure 9 – Quantification of NANOG and SOX17 positive cells in the parthenote embryos. Each point represents one embryo. Kruskal-Wallis test showed no significant difference between expression of NANOG and SOX17 in all groups.*

## 3.3 IL-6 Supplementation and inhibition on *in vivo* embryos

Despite parthenote embryos being a suitable model for mimicking early mammalian development, the absence of a paternal genome contributes to many embryonic abnormalities, including aberrant differentiation and growth in the extra embryonic embryo (Paffoni et al, 2008). In order to assess the role of IL-6 in a fully functional embryo, the above experiments were repeated with embryos collected *ex vivo* at 4-cell to morulae stage, and cultured until E7 in vitro. The embryos were subjected to the treatments at 16-cell to morula stage and maintained until late blastocyst stage (Figure 10).

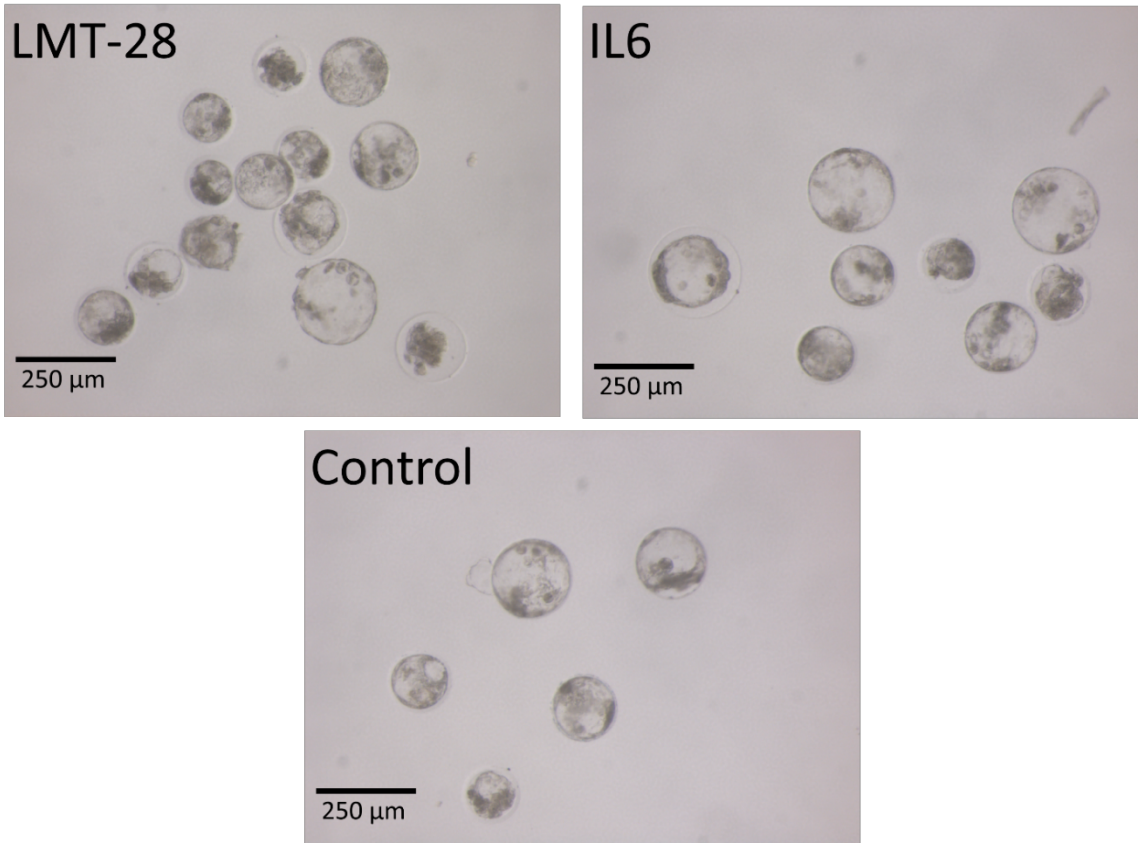



*Figure 10 – Brightfield images of E7 blastocysts prior to fixation.*

Size difference appeared less drastic between the groups in comparison to the parthenote experiment. 70% of LMT-28 group expanded, 63% IL-6 group expanded and 80% of control blastocysts expanded. Expanded IL-6 embryos were slightly bigger than the LMT-28 and control counterparts. 2 LMT-28 blastocysts fully hatched and one control blastocyst had begun the hatching process at the time of fixation.

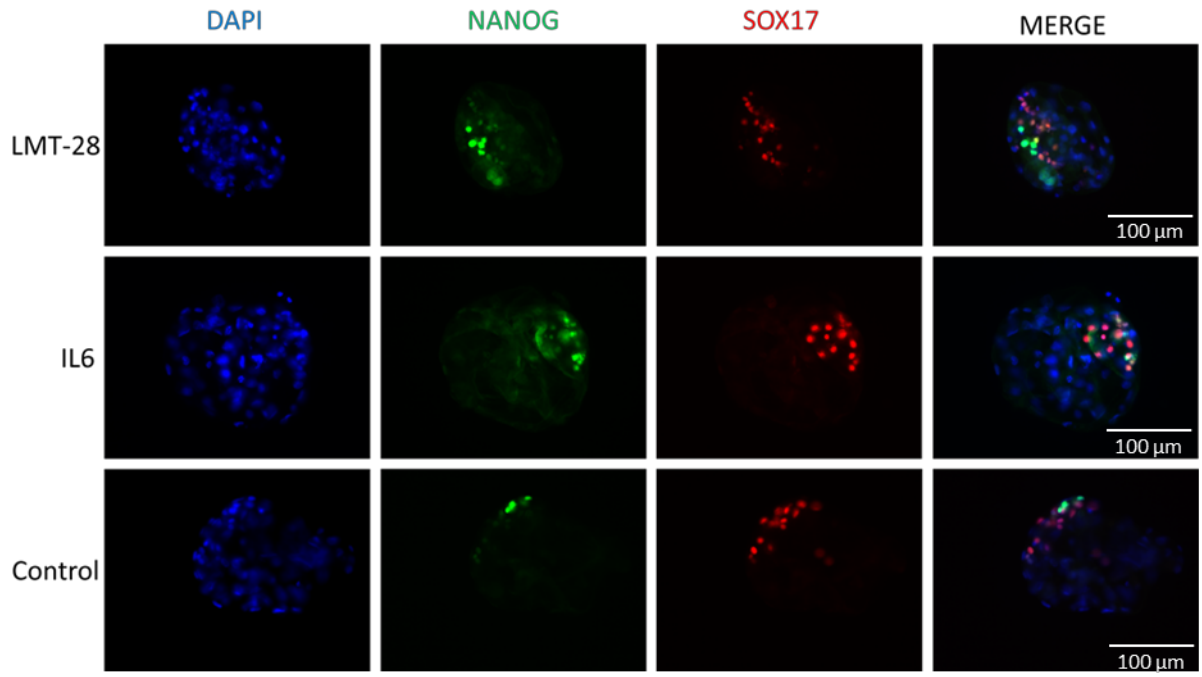



*Figure 11 - Representative immunofluorescence staining images from each of the treatment groups.*

The *in vivo* embryos contained more cells in general than the electrically activated parthenotes. Both ICM and TE cell counts were elevated in comparison (Figure 11, Figure 12).

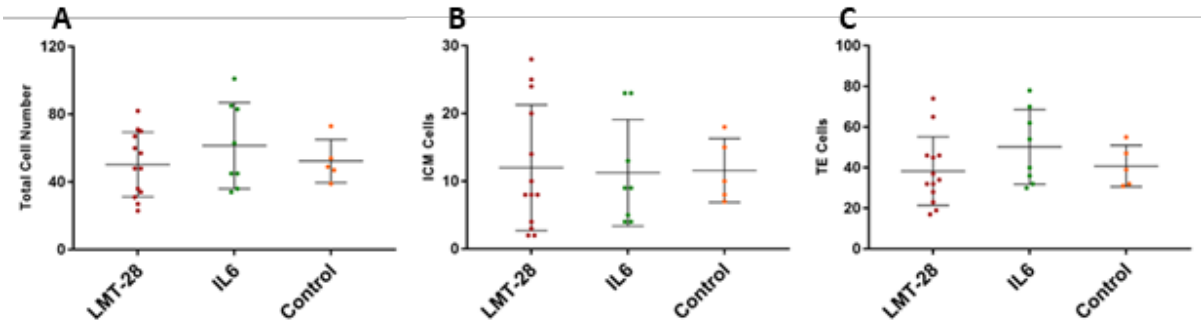



*Figure 12 - Number of cells in the treated in vivo embryos. A) Total cell number of the embryos deduced by all DAPI stained cells. B) ICM population of the embryos deduced by all SOX17 or NANOG positive cells. Costained cells were only counted once. C) TE cell population deduced by subtracting ICM cell number from total cell number. Each point represents one embryo. Statistical analysis by ANOVA determines no significant difference between all groups. Confirmed by post-hoc analysis via Tukey's multiple comparisons analysis.*

ICM:TE ratio was slightly lower in all groups compared to the parthenote counterparts (Figure 13).

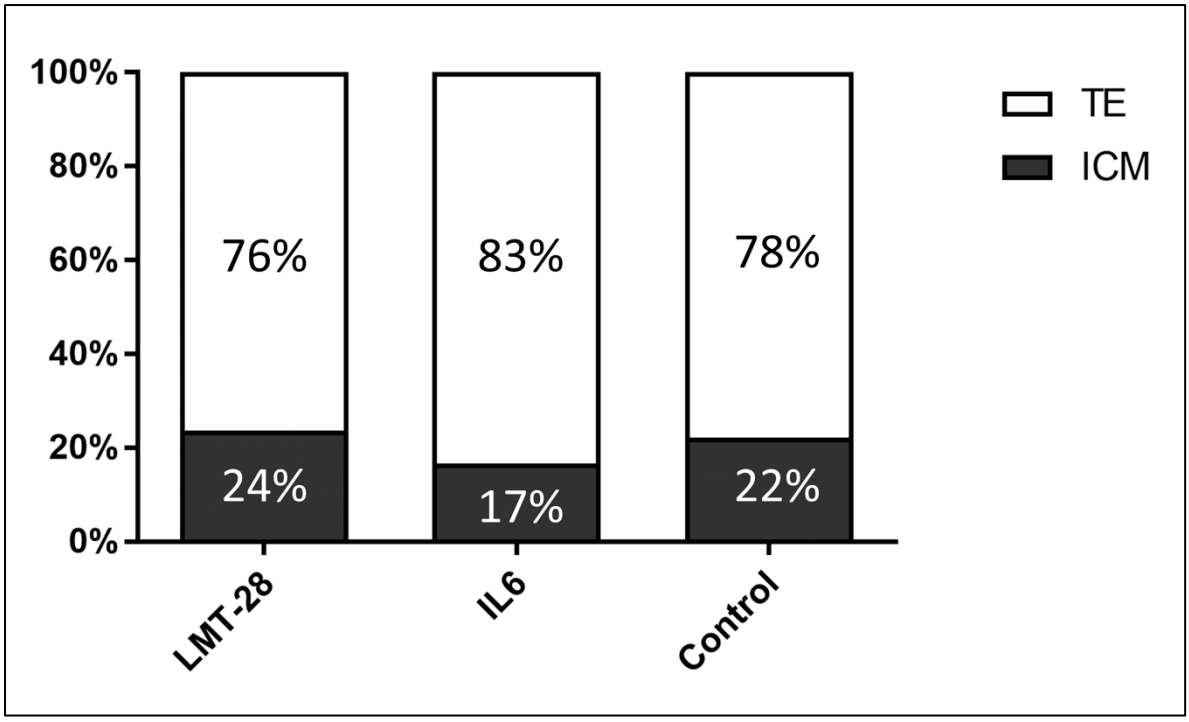



*Figure 13 – ICM:TE ratio percentage mean of the 4 blastocyst groups. No significant difference between the 3 treatment groups and the controls, analysed by Kruskal-Wallis test. The ratio was calculated by dividing NANOG and SOX17 positive cells (ICM) by the number of cells stained with DAPI only (TE).*

As per the parthenote analysis, SOX17 and NANOG expressing cells in each embryo were quantified and plotted onto a scatter graph (Figure 14).

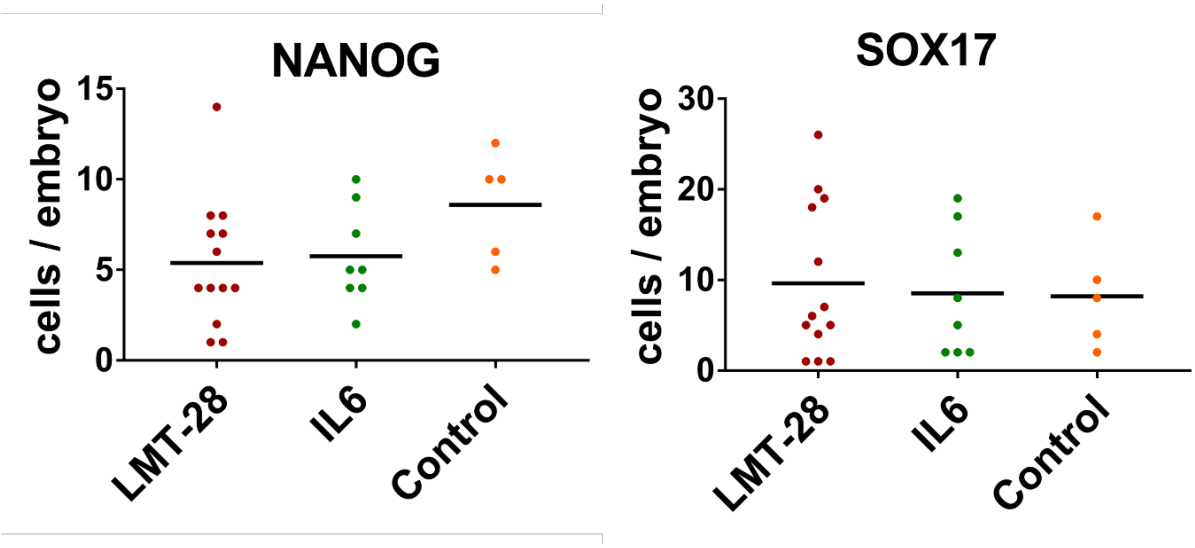



*Figure 14 - Quantification of NANOG and SOX17 positive cells in the in vivo embryos. Each point represents one embryo. As LMT-28 and IL-6 groups are normally distributed in this case, an unpaired t-test was used to determine significance. These was no significant difference between expression of NANOG and SOX17 in the 2 groups.*

## 3.4 IL-6 Knockout Experiments

In order to establish if IL-6 does play a crucial role in the early pig embryo, CRISPR-Cas9 gene editing technique was assess the phenotype of IL-6 null embryos, as knockout of IL-6 could serve as an alternative to the small molecule inhibitor treatment.

Two IL-6 specific guide RNAs were constructed utilising the online CRISPR guide design tool (Hsu et al, 2013), targeting 2 sequences in exon 1. Primers were designed to flank the target sequences (Figure 15).

Guide 1 - CGGGACGCCTGGAAGAAGAT

Guide 2 - CGGCAAAATCTCTGCAATGA

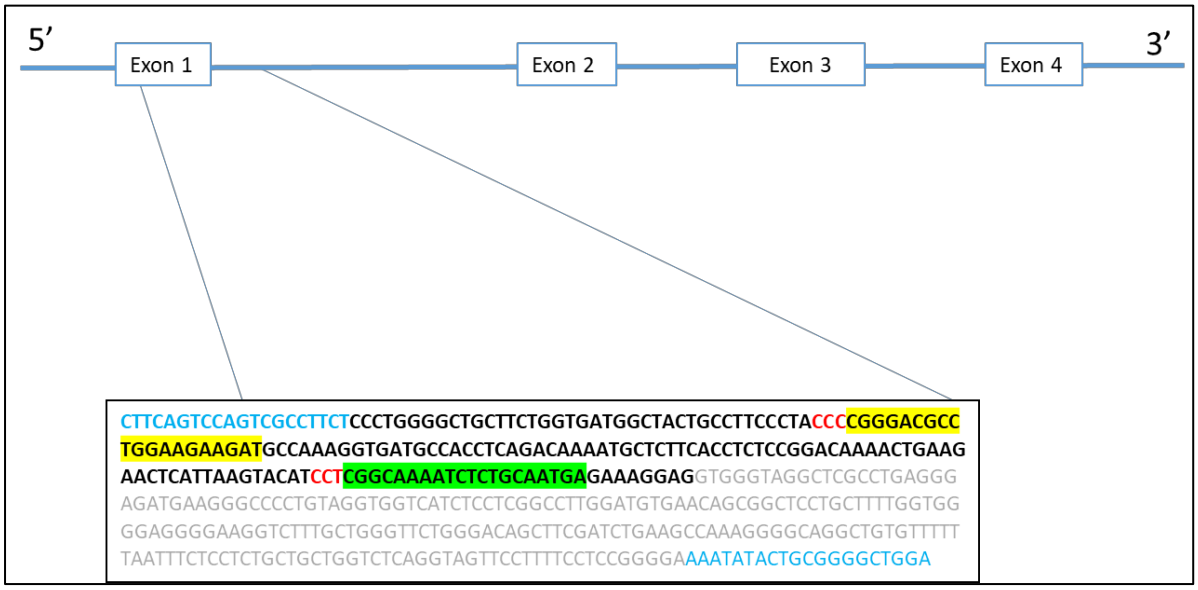



*Figure 15 - Annotated diagram of IL-6 target sequence. Guide targets are highlighted with pam sequences highlighted red. Primers were designed to flank the target sequences and are highlighted blue. Intronic DNA is coloured grey.*

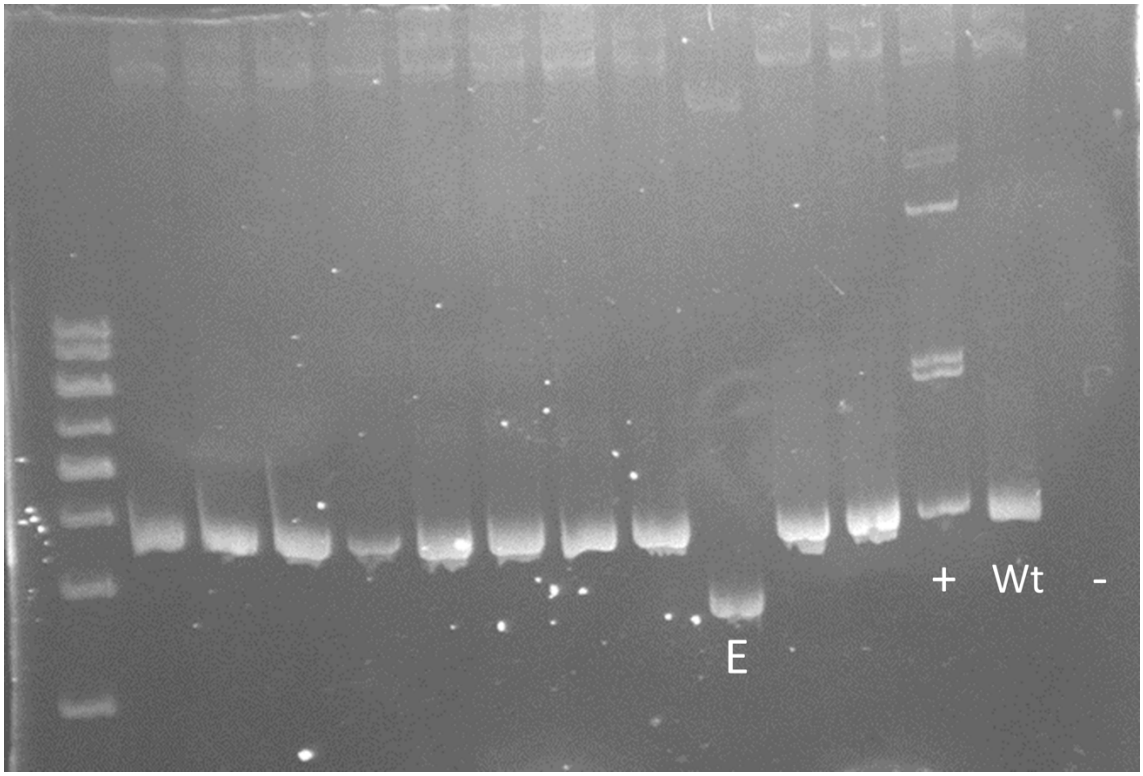



*Figure 16 – Heteroduplex PAGE analysis of presumptive edited blastocysts. Samples annotated with E are confirmed edited by sequencing. Positive, wildtype and negative controls were included on all gels. 1/11 confirmed edited.*

The editing event was confirmed to be a homozygous 96 base pair deletion by sequencing. Prior to being sent for sequencing the presumed edited blastocyst was fixed for IF staining, utilising a method which allows for retrieval after staining for genotyping (Figure 16).

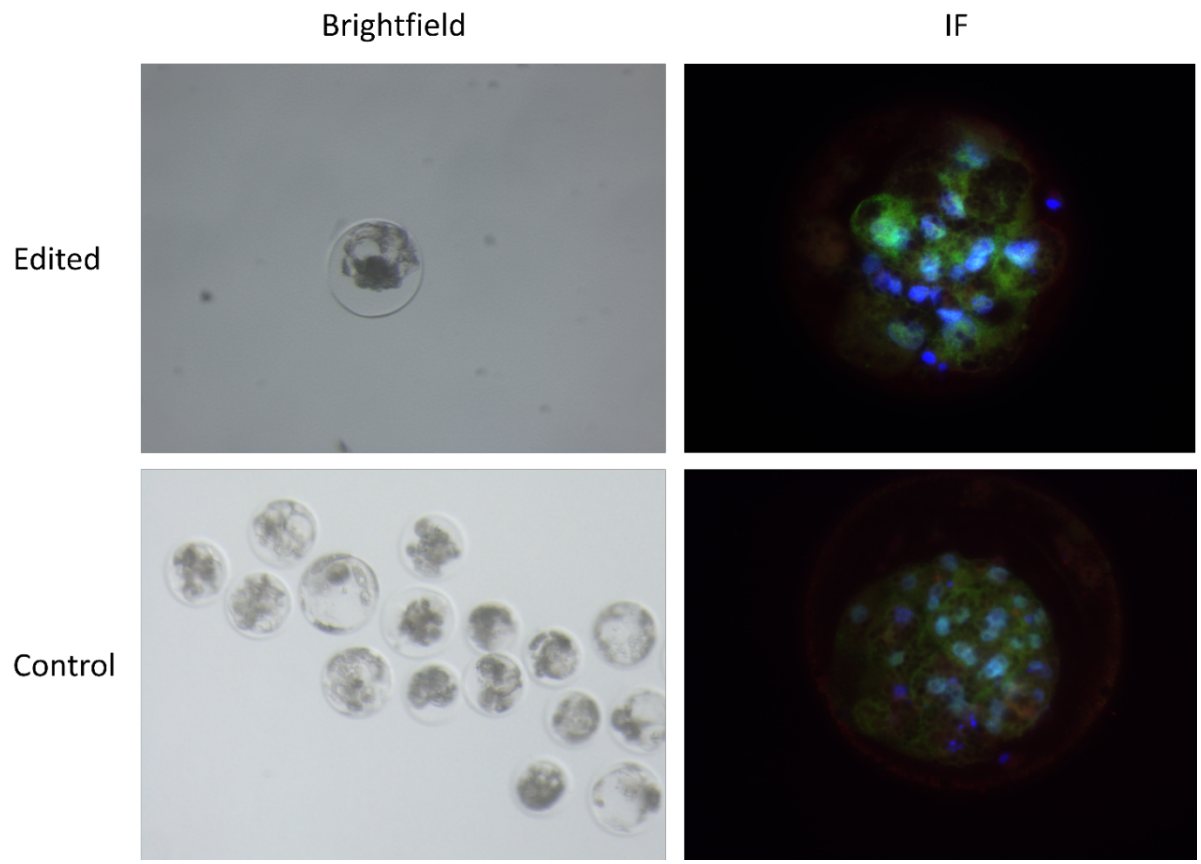



*Figure 17 - Comparison of Edited and control blastocysts prior to staining and after SOX17 and NANOG costaining.*

The staining method for retrieval was not optimised at this point, ultimately resulting in a poor stain with no discernible ICM cells. Total cell number was distinguishable but does not give enough data to understand if IL-6 knockout is creating an aberrant phenotype (Figure 17).

## 3.5 Conclusions

Due to the presence of IL-6 in the early porcine embryo and ICM, paired with lack of LIF and LIFR, I hypothesised that IL-6 was filling the role of LIF in the porcine embryo, in terms of maintaining pluripotency. To investigate this IL-6 and LIF were supplemented to porcine morulae and developed in these conditions to E7 blastocysts. A group of embryos were also subjected to a small molecule IL-6 inhibitor, LMT-28. This investigation was carried out with porcine parthenotes and porcine embryos collected from uterine tracts between the 4-cell stage and morulae.

The parthenote blastocysts exhibited gross morphological abnormalities, with the IL-6 treated group increasing in size and the LMT-28 and LIF groups decreasing in size in comparison to the untreated control group.

Immunofluorescence staining was utilised to determine total cell number, and to quantify ICM and TE cells within each embryo. As ICM was stained with NANOG and SOX17, this gives an insight into the pluripotent state of the embryos, as cells expressing NANOG only are pluripotent and cells expressing SOX17 are differentiating into hypoblast precursors (Ramos-Ibeas et al, 2018). ICM:TE ratio gives an insight into any abnormalities in cell counts as *in vitro* porcine embryos typically have a ratio of 0.3 (Koo et al, 2004).

In the parthenote group there were significant differences between IL-6 and LMT-28, and the IL-6 and LIF groups. IL-6 total cell number and TE cell count was increased in comparison to the LMT-28 group, with no significant changes to the ICM cell count between all groups. This is an indication that IL-6 does have an effect in porcine parthenotes, and seems to exhibit a trophic effect on the TE. The LIF total cell number and TE counts were drastically reduced in comparison to IL-6 treatments, indicating that LIF may possibly have an inhibitory effect on the TE. Total cell counts and TE counts were normally distributed as determined by D'Agostino & Pearson normality test. ANOVA was used to determine significance level, with Tukey's multiple comparisons test as post hoc analysis to determine P values between groups. There was no statistical difference between NANOG and SOX17 cells between treatment groups indicating that IL-6 is not playing a role in maintenance of pluripotency in parthenotes.

As a result of small sample size from the in vivo embryo collection, only LMT-28 and IL-6 treatments were administered alongside an untreated control group.

The embryos collected from uterine tracts displayed morphological differences in terms of blastocyst size between the treatment groups, however the differences were less pronounced

than the parthenote counterparts. The IF staining confirmed that the overall cell counts of the blastocysts were greatly increased in comparison to the parthenote blastocysts at the same embryonic stage.

There were no significant differences in total cell number or ICM/TE cell counts between any of the treatment groups, and no significant difference in the ICM:TE ratios. The SOX17 and NANOG counts were not statistically different, mirroring the parthenote counterparts.

In order to gain a definitive answer into the role of IL-6 in the early embryo, CRISPR-Cas9 genome editing was used to create IL-6 null embryos, and stained to assess cell numbers. To begin this study parthenote embryos were microinjected with gRNA complimentary to porcine IL-6 DNA sequence, alongside Cas9 ribonucleoprotein, as an attempt to reduce mosaicism and increase editing efficiency (Momose et al, 2018; Fogarty et al, 2017). The microinjections gave a yield of 9%, inconsistent with previous results within our laboratory with the same gRNA, indicating operational errors in the microinjection procedure.

Prior to further studies of IL-6 knockouts *in vivo* the knockout efficiency will be increased by continuous study on parthenotes with adjustments to the procedure, to maximise experimental efficiency and yield of edited embryos in order to attain more robust data.

# 4. Eomesodermin Results

EOMES is a transcription factor and has many functions in the developing embryo, particularly throughout gastrulation. In the mouse embryo EOMES plays a role in EMT to allow for migration of cells throughout gastrulation, formation of the mesoderm, definitive endoderm, visceral endoderm and trophectoderm (Arnold et al, 2008). However, the role EOMES carries out in the porcine embryo is not yet clear. Our single cell RNA sequencing (scRNAseq) data showed that EOMES is highly expressed in some E11 porcine epiblasts preceding key mesodermal markers Brachyury (T), FOXA2 and MIXL (Figure 18). This is not the case in the mouse embryo where Eomes is expressed one day after Brachyury expression arises. This indicates that EOMES may play a different and potentially more direct role in mesoderm induction in the gastrulating pig embryo (Rivera-Perez and Magnuson, 2005; Ciruna and Rossant, 1999; Pulina et al, 2015). There is also evidence that EOMES plays a role in the competency of germ cells in humans by inducing SOX17 (Kojima et al, 2017), which is not the case in the murine embryo and supports the hypothesis that the role Eomes carries out during gastrulation is not conserved between the two species.

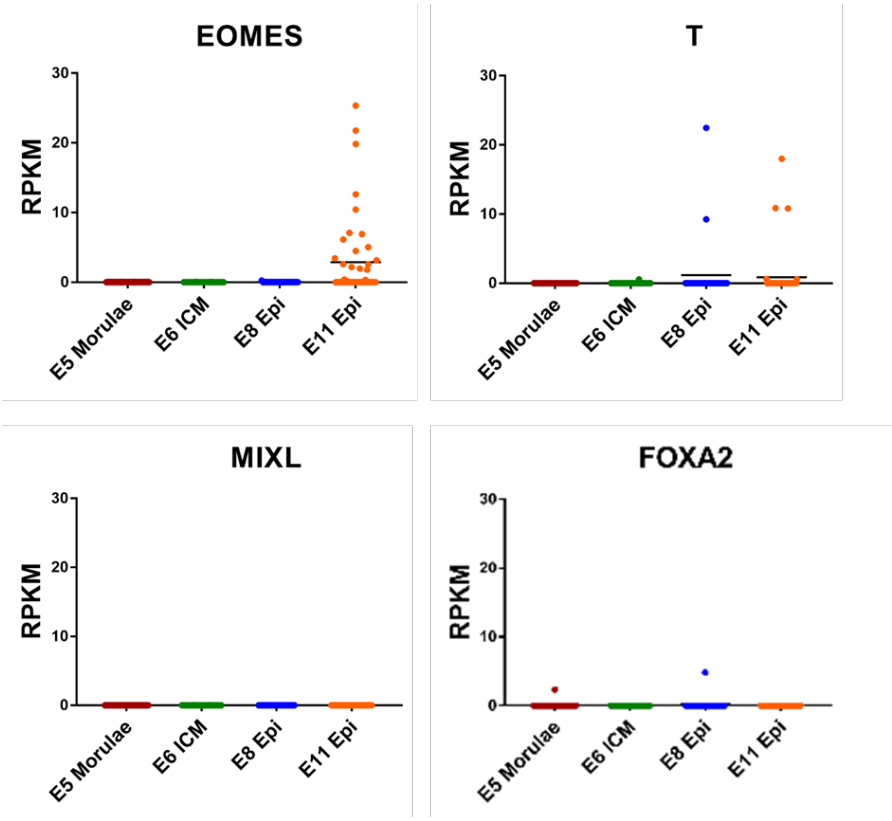



*Figure 18 - dot plots of the expression of key primitive streak and mesendoderm marker genes in differing stages of the pre-primitive streak porcine embryo. RPKM - Reads per kilobase of transcript per million mapped reads.*

EOMES had a higher expression profile in the E11 epiblast in comparison to T and precedes expression of MIXL and FOXA2 at this stage. 20/48 cells measured expressed EOMES at this stage, in comparison to the 5/48 cells expressing T.

To establish the role of eomes in porcine embryos I plan to generate EOMES-null embryos via CRISPR-Cas9 mediated gene editing, and study the phenotype at E9 - E11 *in vivo.* In order to do this 3 gRNAs were selected using a web based CRISPR guide design tool (Hsu et al, 2013), all targeting separate sequences within exon 1. Exon 1 was targeted due to the large size of the exon in comparison to the other 5 exons in the Eomesodermin gene. From exon one the CRISPR tool suggested 3 potential guide RNAs with a target specificity score of over 90% and no exonic off target sequences (Figure 19).

ATGCAGTTAGGGGAGCAGCTCTTGGTGAGCTCGGTGAACCTGCCCGGCGCGCACTTCTACCCGCTGGAGAGT
GCGCGAGGCGGCACCGGCGGGAGCGCCGGGCACCTCCCGGGAGCGGCCCCCTCTCCCCAGAGGCTGGACTTA
GACAAAGCGCCCAAGAAGTTTTCGGGCAGCCTCTCCTGCGAGGCAGGGAGCCGGGAGCCCGCAGCCACCGGC
GCGGGGGCCCCCGCGGCCATGCTCAGTGACGCCGACGCCGGGGACGCCTTTGCCAGCGCTGCGGCGGTGGCC
AAGCCCGGACCCCCGGACGGCCGCAAGGGCTCCCCCTGCGGGGAGGAGGAGCTGCCCTCCGCCGCCGCCGCC
GCCGCCGCAGCTGCCGCGGCCGCCGCTACCGCGCGCTATTCCATGGACAGCCTGAGTTCGGAGCGCTACTAC
CTCCAGTCCCCCGGACCTCAGGGCTCCGAGCTGGCCGCGCCCTGCTCGCTCTTCCCGTACCAGGCGGCAGCT
GGGGCGCCCCACGGATCCGTGTACCCGGCTCCCAACGGGGCGCGCTACCCCTACGGCTCCATGCTGCCCCCC
GGCGGCTTCCCGGCGGCCGTGTGCCCACCCGGGAGGGCGCAGTTCGGCCCGGGAACCGGCGCGAGTAGCGGC
GCGGGAGGCAGCGGCGGCGGGGGAGGCGGCCCGGGCGCCTACCAGTATGGCCAGGGGGCCCCGCTCTACGGG
CCGTACCCCGGGGCGGCAGCGGCGGGTTCCTGCGGAGGATTGGGGGGCCTGGGGGTTCCTGGCTCCGGCTTC
CGTGCCCACGTCTACCTGTGCAACCGGCCTCTGTGGCTCAAATTCCACCGCCACCAAACCGAGATGATCATT
ACGAAACAGGGAAG*GTGAGCGCAGCGCGGAGGGGCCCCGAGGCGTG*GGGGTAAAGAGTGTGTGGTC

*Figure 19 - Annotated sequence of Eomes exon 1. Guide targets are highlighted in blue with pam sequences underlined red. F1R1 primers were designed to flank guide 1 target sequence and is annotated red. F2R2 primers were designed to flank guide 2 and 3 target sequence and is annotated orange. The start of the T-Box sequence is highlighted in purple.*

In order to assess knockout efficiency of our guide RNAs, heteroduplex analysis was carried out on injected embryos. A brief denaturation step creates an open angle between mismatched DNA strands caused by mutations, causing DNA to migrate slower through gels, creating abnormal bands and highlighting embryos that harbour insertions and deletions created by the CRISPR-Cas9 genome editing (Zhu et al, 2014). Large indels were apparent due to change in size of the bands.

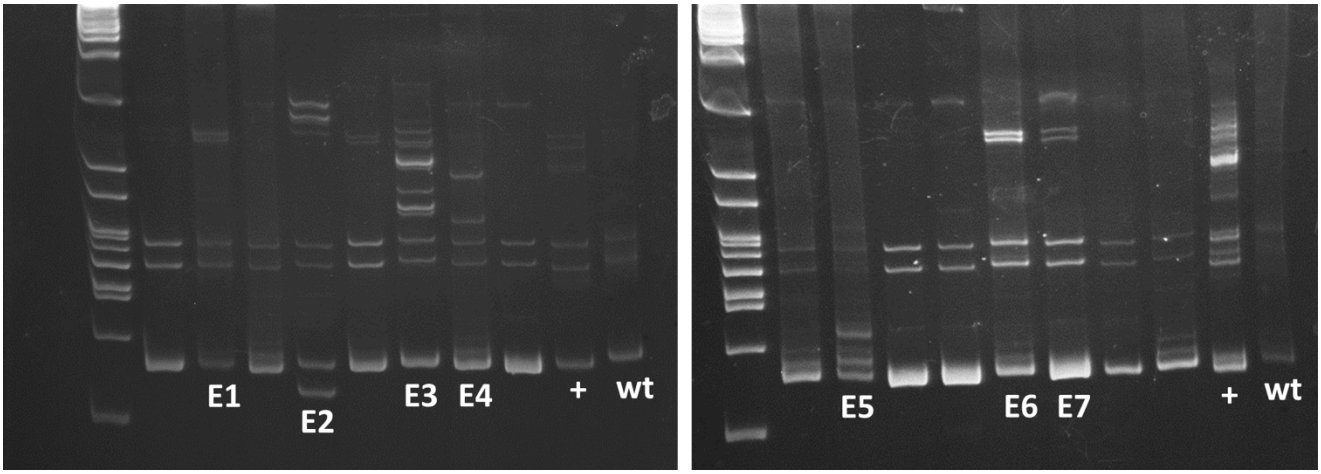



*Figure 20 - Heteroduplex PAGE analysis of guide 1 injected blastocysts. Samples annotated with E are confirmed edited by sequencing. Positive, wildtype and negative controls were included on all gels.*

The types of indel the gRNA created was analysed with an online inference of CRISPR edits (ICE) software tool (Hsaiu et al, 2018). Depicted in figure 3 are representative indels from the 7 guide 1 knockout samples analysed (Figure 21).




*Figure 21 – Representative indels from guide 1 knockout embryos. E2 and E3 show 3 types of indels in the Eomes exon 1, 1 addition and 2 deletions. E4 harbours a homozygous 4bp deletion.*

The ICE tool was also utilised to read the types of mutations and level of mosaicism in each edited embryo. Guide 1 showed a low rate of mosaicism and a range of mutations within each embryo as highlighted in figure 22B.

The guide 1 injected embryos showed a wide range of alleles with no particular trend. The guide 1 and guides 2+3 injections showed an editing efficiency of 44% and 9% respectively, indicating that the guides may not be efficient or injection methodology could be improved (Figure 22A).

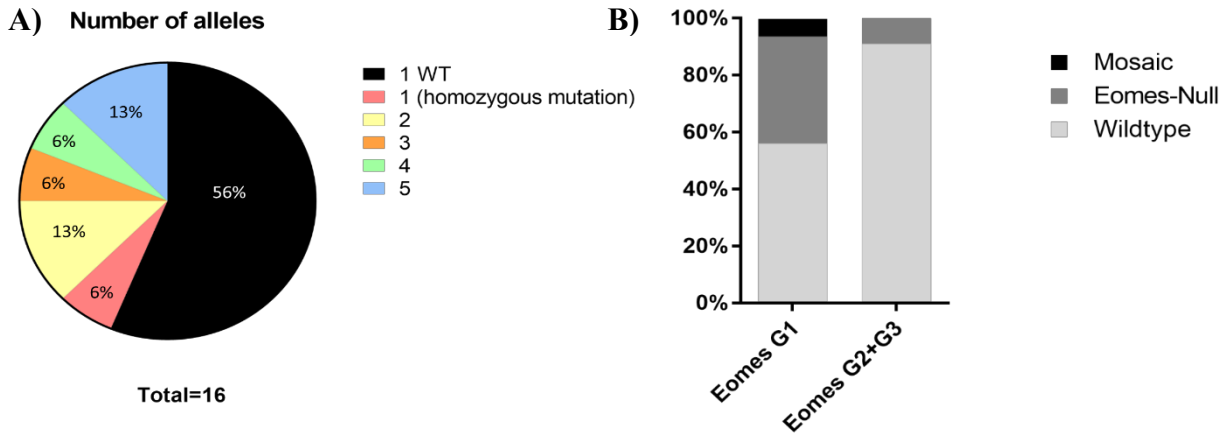



*Figure 12 - A) comparison of mutations found in guide 1 injected pig embryos. B) Proportions of mosaic, Eomes-null or mosaic embryos after microinjection. 1/16 embryos were mosaic for guide 1 injected embryos. 1/12 guide 2+3 injected embryos harboured an editing event, indicating a low guide efficiency.*

Embryo development was a limitation of the injection studies, as parthenogenetically activated blastocyst rate was low. In order to increase yield of blastocysts to gain more robust data on guide efficiency the activation method was optimised. In order to assess changes in developmental rates, lysis was measured at 5 hours post activation, and in later runs cleavage was assessed 1 day post fertilisation.

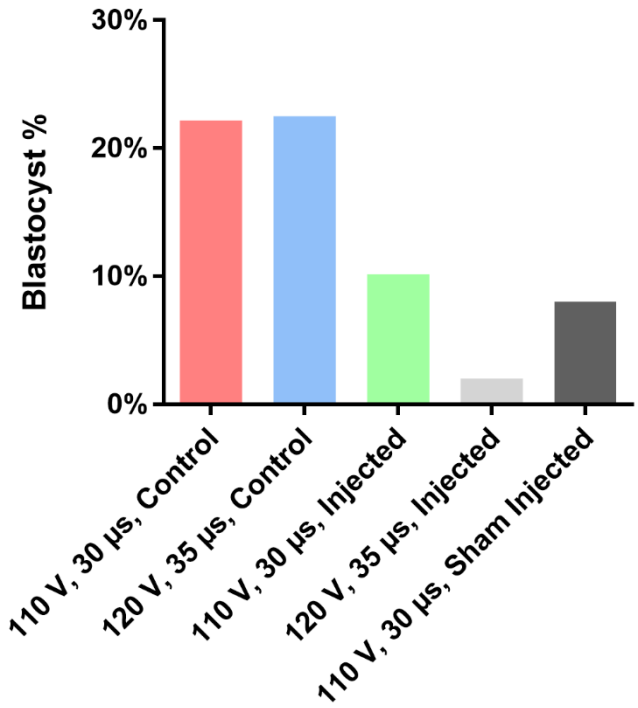



*Figure 23 - Mean blastocyst development rates. Injected groups were injected with Eomes targeting gRNA and sham group was injected with the Cas9 ribonucleoprotein complex in injection buffer. Control groups were activated without injection.*

Activation up until the point of optimisation was performed by subjecting injected oocytes to two, 120 V, 35 µs electric pulses in a 0.5 mm fusion chamber. Reduction of voltage and duration of pulses did not affect uninjected blastocyst development, but improved the blastocyst development of the injected oocytes. Sham injections of Cas9 ribonucleoprotein complex and injection buffer were performed to exclude unspecific effects of the gRNA knockouts on embryonic development, but there was little difference in blastocyst development rates between sham and gRNA injected oocytes under the same activation conditions (Figure 23).

## Conclusions

EOMES was raised as a gene of interest in terms of discerning its role in the developing pig embryo due to our scRNAseq data showing EOMES expression to precede primitive streak formation and expression of mesendodermal markers. Our data showed no notable EOMES expression in ICM or Epiblast until E11, meaning *in vitro* studies of EOMES knockout embryos is not possible as in *vitro* porcine embryos cannot be cultured beyond day 9.

In order to maximise efficiency and embryo yield of *in vivo* experiments, the injection method and gRNA used must have a high survival rate and editing efficiency with a low rate of mosaicism if possible. The aim of reducing mosaicism is to reduce the risk of a variety of phenotypes, some of which may possess mutant alleles and still produce functional proteins. One step incorporated to reduce mosaicism was the use of high concentrations of Cas9 ribonucleoprotein complex, which has been shown to reduce mosaicism and increase editing efficiency in a number of studies (Momose et al, 2018; Fogarty et al, 2017).

The gRNA efficiency at producing knockouts was 46% for guide 1 and 9% for guides 2+3 injected simultaneously. These editing efficiencies were low in comparison to those found in other studies (Fogarty et al, 2017). This low efficiency may be due to the specificity of the gRNA to the target sequence, or potentially due to operational errors during the microinjection procedure. A possible solution to this is to microinject a guide with a known editing efficiency and compare knockouts to rule out operational errors, and retest the current guides designed. If operational error is not the cause of the low editing efficiency, new guides can be produced targeting different sequences within the Eomes gene, until a sufficient editing efficiency is reached. However, target sequences within the genes are limited due to PAM free regions within DNA (PAM sites being a requirement for Cas9 binding) and new gRNAs may also have some degree of off target specificity (Zhao et al, 2017).

In order to generate a large amount of embryos to gain significant data on the knockout studies, the embryo activation method was optimised to increase yield. Historically, pig embryos generated with parthenogenetic activation develop better than those produced by IVF, and therefore I opted for the former to study gRNA efficiency. The preliminary optimisation with uninjected oocytes showed 2 pulses at 120 V, 35 µs to be more efficient for creating blastocysts. However for injected oocytes, these conditions reduced final blastocyst development in comparison to 110 V, 35 µs for 2 pulses. This setting was adopted for the rest of the activation experiments. The increase in final blastocyst percentage may have been due

to more gentle conditions on the oocytes, which are fragile and more prone to lysis after injection. A sham injection group was also incorporated, consisting of Cas9 ribonucleoprotein complex and Tris-injection buffer to determine if embryonic lethality was being caused by the gene editing machinery. There was little difference between guide injected and sham injected embryos, indicating no embryonic lethality caused by knockouts. Furthermore, no gene editing events took place in the sham injected embryos.

# 5. Discussion

The aim of this study was to establish the role of 2 genes, Interleukin-6 (IL-6) and Eomesodermin (EOMES), in the early development of the porcine embryo. My first hypothesis was that IL-6 plays a role in maintenance of pluripotency within the porcine blastocyst. The second hypothesis was that EOMES plays a different role during gastrulation in pigs than in mice.

In order to test the first hypothesis IL-6 was both blocked and supplemented to embryos *in vitro* to assess effects on embryonic growth and proliferation of the 2 cell populations within the blastocyst, the ICM and TE. CRISPR-Cas9 mediated IL-6 knockout experiments were also planned to gain a definitive insight into the role of IL-6 in the blastocyst. To test the second hypothesis I planned to create EOMES knockout embryos by CRISPR-Cas9 gene editing, and transfer the embryos into sows to gestate until E11, the point at which EOMES is expressed at a high level in the porcine embryo. Due to time constraints and optimisation issues with the process of generating knockout embryos, I was unable to conduct the embryo transfer experiment.

In the next section I will discuss the procedures and results of this study and present my findings with regards to the role of IL6 and EOMES in the preimplantation embryo.

## 5.1 Understanding the role of Interleukin-6 in the developing pig embryo

The finding that IL-6 is present in the mouse embryo was first published in 1992, however its function is still yet to be understood (Lee, 1992). Single cell RNA sequencing of porcine embryos at various stages showed IL-6 to be expressed at high levels in E5 morulae and E6 TE cells. Furthermore, IL-6 receptor (IL6R) expression is mainly present in the ICM, suggesting that IL-6 is secreted from the TE and may bind to receptors on the ICM in a paracrine fashion. To support this theory, IL6ST, a pleiotropic signal transducing subunit of IL6R is also highly expressed in E6 ICM, but is also present in all measured stages of the embryo. IL6ST binds LIF which activates Stat3, a signalling pathway involved in the induction of both pluripotency genes and TE genes such as Cdx2 and Tfap2c in mouse embryonic stem cells (mESCs), which also plays a role in cell proliferation via inhibition of apoptosis (Tai, Schulze and Ying, 2014; Shen et al, 2012). Interestingly LIF is not expressed in the early pig embryo at any stage leading to the hypothesis that IL-6 may be filling the role of LIF in terms of maintaining pluripotency in the pig embryo.

To test this hypothesis *in vitro,* groups of E5 parthenote embryos were supplemented with IL-6 and LIF, and also subjected to a small molecule inhibitor (LMT-28), a specific inhibitor of IL-6 (Hong et al, 2015). The embryos were cultured in their respective conditions until late E6-E7, at which point they were collected and stained for analysis. The expanded blastocysts in the IL-6 group appeared greater in size than all other groups whereas the expanded blastocysts in the LMT-28 group appeared slightly smaller than the controls. Interestingly the LIF group had the least growth, with all blastocysts, including the expanded being severely stunted. The IF pictures and cell counts confirmed these observations, as there was significant difference between the total cell numbers of embryos cultured in the presence of IL-6 and LMT-28 (P=0.0157), and significant difference between the total cell numbers of IL-6 and LIF groups (P=0.0069), with blastocysts cultured in the presence of IL-6 displaying more cells than the other groups. In addition the TE cell counts displayed significant differences between the same groups (P=0.0058 and P=0.0005 respectively). There were no significant differences in the ICM cell counts between all groups. This data suggests that IL-6 has a trophic effect on the TE cells and LIF is having an inhibitory effect on the expansion of the TE. The finding that IL-6 increases the cell number of the TE partly coincides with a study which states IL-6 increases cell number by inhibition of apoptosis in porcine parthenote embryos. However, despite using the same concentration of IL-6 (10ng/µl) the study also reported an increase in size of the ICM which was not apparent in our study (Shen et al, 2012). Additionally, previous studies of porcine blastocysts cultured in LIF from the 4-8 cell stage report fewer blastocysts developed but no apparent change to the cell numbers of the blastocysts (Eckert, Tao and Niemann, 1997). This could be due to a difference in signalling mechanisms and gene expression between in vivo embryos and parthenotes (Gomez et al, 2009), although further work would need to be conducted to confirm this. LIF appears to be inhibiting TE expansion, potentially by interfering IL-6 signalling. One study reported downregulation of IL6R by LIF in mouse leukaemic cells, but there is no evidence of this taking place in the early embryo (Yamaguchi et al, 1992).

To assess if IL-6 supplementation/inhibition had an effect on the pluripotent state of the embryo, the blastocysts were stained for NANOG and SOX17. Blastocysts expressing NANOG only were deemed as pluripotent, and SOX17 expression is a marker of hypoblast lineage. Epiblast lineage could be determined by NANOG positive, SOX17 negative cells in embryos positive for both stains (Ramos-Ibeas et al, 2018). There was no significant difference between

number of NANOG positive cells and number of SOX17 positive cells per blastocyst between treatments, implying that the role of IL-6 in parthenogenetic embryos is to enhance the development of the trophectoderm lineage, with no direct effect on the ICM.

Despite parthenotes being an easy to access model for mimicking early mammalian embryonic development in vitro, the absence of a paternal genome leads to abnormalities within the embryos in terms of differentiation and proliferation of embryonic cells (Paffoni et al, 2008). Embryos cultured *in vitro* also display altered gene expression in comparison to in vivo counterparts (Niemann and Wrenzycki, 2001). Additionally, parthenotes display a higher degree of apoptosis than IVF counterparts (Hao et al, 2004). To fully understand the role of IL-6 in the preimplantation pig embryo the above experiment was repeated with embryos collected from artificially inseminated sows. Due to a small number of embryos collected the LIF group was excluded from the *in vivo* study to allow for more robust data in the IL-6 and LMT-28 groups.

The brightfield images of the E7 embryos showed a less drastic morphological changes in comparison to the parthenote counterparts. The expanded embryos from the IL-6 culture group were slightly larger than the LMT-28 and control expanded blastocysts, however there was little observable difference between the LMT-28 and control group. Despite the IL-6 embryos appearing slightly larger there was no significant difference between the total cell number, ICM cell count and TE cell count between any of the groups. All 3 cell counts were higher than the parthenote cell counts, which may be explained by increased apoptosis in parthenotes and the fact that embryos cultured *in vitro* have retarded development in comparison to *in vivo* embryos (Macahaty, Day and Prather, 1998). As the majority of the embryos were collected from uterine tracts at 16-cell and morula stage and cultured *in vitro* for 3 days, these issues in development were less pronounced. The increased cell numbers in the *in vivo* blastocysts could potentially offer an explanation for the decreased effect the treatments had on the blastocysts, as increased cell numbers suggest that *in vivo* embryos are of much higher quality and may be less susceptible to the effects of the treatments (Hoelker et al, 2009). Another possible explanation would be that an increase of IL-6 in the blastocyst microenvironment as a result of the increased cell numbers, leading to reduction in efficiency of the IL-6 inhibitor.

The ICM:TE ratio was slightly lower in all groups in comparison to the parthenote counterparts. Whereas the cell count differences correlate with published literature, the

ratios of ICM:TE in porcine embryos collected *in vivo* were expected to be higher (Machaty, Day and Prather, 1998). There was no significant difference in the ratios between the groups indicating that the treatments had no profound effect on the two cell populations within the blastocysts.

As reported with the parthenote treatments, the *in vivo* embryos displayed no significant difference between the number of cells expressing NANOG and SOX17 between the treatments, implying that IL-6 does not have an effect on the pluripotent cells of the pig embryo.

As the concentration of the LMT-28 used in the parthenote study (30µM) was enough to induce an observable effect on the embryos, this concentration was also adopted for the *in vivo* study. However as previously discussed, this concentration may not have been sufficient to block IL-6 in the *in vivo* embryos due to high quality of the embryos and possibly increased concentrations of IL-6 inside the embryos due to higher cell count. One way to validate the differences between the parthenotes and in vivo embryos would be to repeat the in vivo experiment with a series of increased concentrations of LMT-28 to assess if there are any changes to the cell numbers at higher concentrations. Another viable route to assess IL-6 activity in the preimplantation embryo is gene knockout by CRISPR-Cas9.

I planned to assess the phenotype presumptive IL-6 knockout embryos by staining as per the previous study, with the additional step of retrieval of the embryos after staining to analyse editing events by PCR and sequencing. These methods were first tested on parthenotes to ensure a high editing efficiency and blastocyst survival rate. The adapted method for staining to allow for retrieval and genotyping was not yet practiced or optimised by myself, causing issues with the staining and overall efficiency of this experiment. Knockout efficiency of IL-6 was also poor in comparison to previous members of our laboratory, indicating operational issues in the microinjection technique. Optimisation of the microinjection technique will be further discussed in the next section of this chapter.

## 5.2 Understanding the role of EOMES in the gastrulating pig embryo

EOMES was chosen as a gene of interest in light of the finding that EOMES is highly expressed in the porcine epiblast, and expression precedes that of T. This contrasts with expression in the mouse embryo as T expression is present in the pre-streak mouse epiblast one day before expression of EOMES arises (Rivera-Perez and Magnuson, 2005; Ciruna and Rossant, 1999).

Porcine EOMES also precedes MIXL expression, which is not the case in the mouse embryo, where MIXL expression also precedes EOMES expression by a day (Pulina et al, 2015).

In order to elucidate the role of EOMES in the pig embryo, I planned to create EOMES knockout embryos by CRISPR-Cas9 gene editing, and to study the phenotype at E11, early somites and late somites stages, in order to fully elucidate the function of EOMES in the mesendoderm. Due to the small number of embryos likely to be collected for the *in vivo* embryo transfer study, the gene editing technique was to be optimised to maximise editing efficiency and to increase rates of embryo survival after the microinjection procedure.

To maximise the likelihood of finding an efficient guide RNA (gRNA) to facilitate the EOMES knockout, 3 gRNAs were designed with an online CRISPR design tool (Hsu et al, 2013), all of which displayed high specificity for the target sequence and no exonic off targets. The guides were produced through a cloning method for the first batch, and the second batch were synthesised with a cloning free column kit. The efficiency of the guides at producing knockout embryos was tested by microinjecting *in vitro* oocytes followed by parthenogenetic activation and culture to blastocyst. Combinations of guides were also tested after a report stated injections of multiple gRNAs targeting one gene increases editing efficiency (Zhou et al, 2014). The embryos were cultured until E6-E7 blastocysts, processed and sent for sequencing to assess for mutations.

The mutation spectrum was analysed not only to give a percentage success rate of the gRNAs, but also was used to analyse any mosaicism, otherwise termed monoallelic mutations, which can lead to embryos containing populations of mutant and wildtype cells. Mosaic embryos are not ideal for this type of study as wildtype populations of cells in embryos are still express the functional targeted gene (Zuo, Cai and Yang, 2017). In order to reduce mosaicism direct injections of Cas9 ribonucleoprotein complex were used (Fogarty et al; 2017; Momose et al, 2018; Yen et al, 2014), alongside injection of multiple gRNAs (Zuo, Cai and Yang, 2017). The use of Cas9 ribonucleoprotein in place of Cas9 mRNA reduced risk of mosaicism as the time taken for RNA translation into functional Cas9 protein may take place after the first cell division, ultimately leading to cells in the early embryo harbouring different mutations (Hashimoto, Yamashita and Takemoto, 2016).

From 16 embryos analysed, injections of guide 1 gave an editing efficiency of 44%, with only 6% of embryos harbouring both wildtype and mutant alleles. Guide efficiency of guides 2 and 3 injected simultaneously produced one edited embryo from 12 injected blastocysts, giving

an editing efficiency of 8%. This editing rate is relatively low in comparison to other reported studies (Fogarty et al, 2018) and could be due to the nature of the gRNA itself or errors in the microinjection procedure. A test to rule out operational error would be to inject a guide with an already established editing efficiency and make tweaks to the method until the efficiency is matched. If methodological error is ruled out a number of adjustments could be made to the manner in which gRNAs are introduced, failing that new guides could be constructed and tested. One possible change would be to modify the concentration of the gRNA and the ribonucleoprotein complexes introduced to the embryos. There is evidence that increasing gRNA-Cas9 concentrations can raise editing efficiency, but higher Cas9 concentrations can tolerate mismatches within the target site leading to off target cleavage, therefore an increase in concentration could cause the efficiency of the EOMES specific guides to increase, but may also add an extra issue in terms of off target editing events (Pattanayak et al, 2013; Hsu et al, 2013).

Overall, the blastocyst yield from these experiments was very low and it took a considerable amount of time to gather enough embryos to be screened for mutations. In order to gain more robust data to understand the efficiency of the guides, the injection and activation method was optimised to increase blastocyst yield. Despite the low yield of blastocysts from parthenogenetic activation this method of  was continued through the optimisation due to low blastocyst rates associated with porcine IVF and issues with polyspermic embryos, which often do not develop to blastocyst stage and can create allelic complexity, affecting the efficiency of CRISPR-Cas9 mediated gene editing (Kikuchi, 2004; Liang et al, 2015).  In a strategy to increase the blastocyst rate of activated oocytes, the activation parameters were adjusted and a lower volume of injection buffer (TE buffer, Cas9-gRNA complex) was injected, to minimise lysis throughout the activation process (Doe, Brown and Boroviak, 2018). The voltage and duration of electrical pulses during the activation was also reduced from 2 pulses at 120V, 35µs to 2 pulses at 110V, 30µs in order to subject the fragile post-injection embryos to more gentle stimuli. The post activation treatment of cytochalasin B and 6-DMAP remained the same across all groups. Cytochalasin B was applied to inhibit extrusion of a second polar body, leading to a more developmentally competent diploid parthenote, and 6-DMAP also prevents the extrusion of the second polar body by inhibition of the MAPK signalling pathway (Grupen et al, 2002; Yi and Park, 2005). The uninjected parthenotes showed no major difference in developmental rates between the 2 activation settings. The injected

parthenotes were decreased in comparison to the uninjected group, and the decrease in voltage and pulse duration had a positive effect on the blastocyst yield in comparison to the injected group activated at 120V for 35µs. A sham injection group was also set up to assess if the potential genome editing was causing a decrease in blastocyst yield. The sham injection consisted of the Cas9 ribonucleoprotein in TE buffer and absence of gRNA. The sham group displayed the same developmental rate as the injection group, indicating that gene editing is not causing embryonic lethality, and the reduction in blastocyst yield between uninjected controls and the injected group is due to fragility of embryos after injection, or possible cytotoxic effects of the Cas9 ribonucleoprotein-TE buffer, which has not been reported in the literature.

Prior to the in vivo assessment of EOMES function in the porcine embryo by CRISPR-Cas9 mediated EOMES knockout, further investigation will need to be done in terms of optimising guide efficiency and development of microinjection technique. A second method of gene editing zygotes could also be tested as there have been reports of efficient genome editing of mouse zygotes by electroporation methods (Chen et al, 2016; Hashimoto and Takemoto, 2015; Qin et al; 2015). However, successful CRISPR delivery by electroporation in porcine embryos has not been reported and may take a considerable amount of time to develop an efficient method with editing efficiencies comparable to injections.

## 5.3 Conclusions

The work carried out throughout this project has led me to draw conclusions regarding the role of IL-6 in the preimplantation embryo, the methodology of this work and adjustments I can make in future experiments, and the overall scope of future work in this area.

1) IL-6 has a trophic effect on the trophectoderm lineage of *in vitro* parthenogenetically activated embryos.

2) LIF has an inhibitory effect on the expansion of the TE lineage in blastocysts in parthenotes.

3) Further optimisation of our parthenogenetic activation and embryo culture is necessary in order to maximise embryo yield and gain more robust data regarding our CRISPR experiments. Additionally, adjustments need to be made to my microinjection technique to maximise gene editing efficiency, while minimising embryonic lethality.

This optimisation is necessary prior to any *in vivo* CRISPR studies due to the costly and time consuming nature of the work, making repeat experiments difficult.

## 5.4 Future work

Further work is needed to understand if IL-6 and LIF exhibit the same role in viable *in vivo* embryos as observed in the parthenotes. The experiments should be repeated with adjustments as listed above with a greater sample size as to maximise the power of statistical analysis. In this study the untreated control groups for both parthenote and in vivo groups were small and no conclusions could be drawn from the results of the control groups by statistical analysis.

As mentioned previously in this chapter, once the gene editing methods have been aptly optimised the function of EOMES in the porcine embryo can be investigated. As EOMES is expressed at embryonic day 11, this study is beyond the scope of in vitro work and would require the transfer of edited embryos to sows to be retrieved after day 11. As there is no evidence of how EOMES knockout would affect the embryo the best course of action would be to transfer a batch of edited embryos to a number of sows and retrieve them at different time points, for example E11-12 at the start of gastrulation, E12-13 early somites and the late somites stages (Hassoun et al, 2010). This would give a comprehensive insight into the effect that EOMES knockout has on the pig mesendoderm and if removal of EOMES causes embryonic lethality.

# DECLARATION

I declare that this thesis was composed by myself, that the work contained within is my own except where stated otherwise in the text. This work has not been submitted for any other degree or award.

# 6. Bibliography

Akdis, M., S. Burgler, R. Crameri*, et al.* 2011. 'Interleukins, from 1 to 37, and interferon-gamma: receptors, functions, and roles in diseases', *J Allergy Clin Immunol*, 127: 701-21 e1-70.

Alexander, J., and D. Y. Stainier. 1999. 'A molecular pathway leading to endoderm formation in zebrafish', *Curr Biol*, 9: 1147-57.

Arkell, R. M., N. Fossat, and P. P. Tam. 2013. 'Wnt signalling in mouse gastrulation and anterior development: new players in the pathway and signal output', *Curr Opin Genet Dev*, 23: 454-60.

Arnold, S. J., U. K. Hofmann, E. K. Bikoff*, et al.* 2008. 'Pivotal roles for eomesodermin during axis formation, epithelium-to-mesenchyme transition and endoderm specification in the mouse', *Development*, 135: 501-11.

Arnold, S. J., J. Sugnaseelan, M. Groszer*, et al.* 2009. 'Generation and analysis of a mouse line harboring GFP in the Eomes/Tbr2 locus', *Genesis*, 47: 775-81.

Artus, J., A. Piliszek, and A. K. Hadjantonakis. 2011. 'The primitive endoderm lineage of the mouse blastocyst: sequential transcription factor activation and regulation of differentiation by Sox17', *Dev Biol*, 350: 393-404.

Babiarz, B. S., L. C. Romagnano, and G. M. Kurilla. 1992. 'Interaction of mouse ectoplacental cone trophoblast and uterine decidua in vitro', *In Vitro Cell Dev Biol*, 28A: 500-8.

Babon, J. J., I. S. Lucet, J. M. Murphy*, et al.* 2014. 'The molecular regulation of Janus kinase (JAK) activation', *Biochem J*, 462: 1-13.

Batlle, E., E. Sancho, C. Franci*, et al.* 2000. 'The transcription factor Snail is a repressor of E-cadherin gene expression in epithelial tumour cells', *Nature Cell Biology*, 2: 84-89.

Beisaw, A., P. Tsaytler, F. Koch*, et al.* 2018. 'BRACHYURY directs histone acetylation to target loci during mesoderm development', *EMBO Rep*, 19: 118-34.

Ben-Haim, N., C. Lu, M. Guzman-Ayala*, et al.* 2006. 'The nodal precursor acting via activin receptors induces mesoderm by maintaining a source of its convertases and BMP4', *Dev Cell*, 11: 313-23.

Bjornson, C. R., K. J. Griffin, G. H. Farr, 3rd*, et al.* 2005. 'Eomesodermin is a localized maternal determinant required for endoderm induction in zebrafish', *Dev Cell*, 9: 523-33.

Burtscher, I., and H. Lickert. 2009. 'Foxa2 regulates polarity and epithelialization in the endoderm germ layer of the mouse embryo', *Development*, 136: 1029-38.

Camus, A., A. Perea-Gomez, A. Moreau*, et al.* 2006. 'Absence of Nodal signaling promotes precocious neural differentiation in the mouse embryo', *Dev Biol*, 295: 743-55.

Chapman, J. R., M. R. Taylor, and S. J. Boulton. 2012. 'Playing the end game: DNA double-strand break repair pathway choice', *Mol Cell*, 47: 497-510.

Chazaud, C., Y. Yamanaka, T. Pawson*, et al.* 2006. 'Early lineage segregation between epiblast and primitive endoderm in mouse blastocysts through the Grb2-MAPK pathway', *Dev Cell*, 10: 615-24.

Chen, D., W. Liu, A. Lukianchikov*, et al.* 2017. 'Germline competency of human embryonic stem cells depends on eomesodermin', *Biol Reprod*, 97: 850-61.

Chen, S., B. Lee, A. Y. Lee*, et al.* 2016. 'Highly Efficient Mouse Genome Editing by CRISPR Ribonucleoprotein Electroporation of Zygotes', *J Biol Chem*, 291: 14457-67.

Chi, L., U. Saarela, A. Railo*, et al.* 2011. 'A secreted BMP antagonist, Cer1, fine tunes the spatial organization of the ureteric bud tree during mouse kidney development', *PLoS One*, 6: e27676.

Cho, S. W., J. Lee, D. Carroll*, et al.* 2013. 'Heritable gene knockout in Caenorhabditis elegans by direct injection of Cas9-sgRNA ribonucleoproteins', *Genetics*, 195: 1177-80.

Content, J., L. Dewit, D. Pierard*, et al.* 1982. 'Secretory Proteins Induced in Human-Fibroblasts under Conditions Used for the Production of Interferon-Beta', *Proceedings of the*

*National Academy of Sciences of the United States of America-Biological Sciences*, 79: 2768-72.

Costello, I., I. M. Pimeisl, S. Drager*, et al.* 2011. 'The T-box transcription factor Eomesodermin acts upstream of Mesp1 to specify cardiac mesoderm during mouse gastrulation', *Nat Cell Biol*, 13: 1084-91.

Doe, Brendan, Ellen Brown, and Katharina Boroviak. 2018. 'Generating CRISPR/Cas9-Derived Mutant Mice by Zygote Cytoplasmic Injection Using an Automatic Microinjector', *Methods and Protocols*, 1: 5.

Dorey, K., and E. Amaya. 2010. 'FGF signalling: diverse roles during early vertebrate embryogenesis', *Development*, 137: 3731-42.

Doudna, J. A., and E. Charpentier. 2014. 'Genome editing. The new frontier of genome engineering with CRISPR-Cas9', *Science*, 346: 1258096.

Fogarty, Norah M. E., Afshan McCarthy, Kirsten E. Snijders*, et al.* 2017. 'Genome editing reveals a role for OCT4 in human embryogenesis', *Nature*, 550: 67.

Gadue, P. et al, 2006. Wnt and TGF-β signaling are required for the induction of an *in vitro* model of primitive streak formation using embryonic stem cells. *PNAS.* 103;45. 16806-16811

Gearing, D. P., C. J. Thut, T. Vandenbos*, et al.* 1991. 'Leukemia Inhibitory Factor Receptor Is Structurally Related to the Il-6 Signal Transducer, Gp130', *Embo Journal*, 10: 2839-48.

Gerwin, N., G. Q. Jia, R. Kulbacki*, et al.* 1995. 'Interleukin gene expression in mouse preimplantation development', *Dev Immunol*, 4: 169-79.

Gomez, E., A. Gutierrez-Adan, C. Diez*, et al.* 2009. 'Biological differences between in vitro produced bovine embryos and parthenotes', *Reproduction*, 137: 285-95.

Grupen, C. G., J. C. Mau, S. M. McIlfatrick*, et al.* 2002. 'Effect of 6-dimethylaminopurine on electrically activated in vitro matured porcine oocytes', *Mol Reprod Dev*, 62: 387-96.

Guillomot, M., A. Turbe, I. Hue*, et al.* 2004. 'Staging of ovine embryos and expression of the T-box genes Brachyury and Eomesodermin around gastrulation', *Reproduction*, 127: 491-501.

Gupta, A., V. L. Hall, F. O. Kok*, et al.* 2013. 'Targeted chromosomal deletions and inversions in zebrafish', *Genome Res*, 23: 1008-17.

Gupta, R. M., and K. Musunuru. 2014. 'Expanding the genetic editing tool kit: ZFNs, TALENs, and CRISPR-Cas9', *J Clin Invest*, 124: 4154-61.

Hai, T., F. Teng, R. Guo*, et al.* 2014. 'One-step generation of knockout pigs by zygote injection of CRISPR/Cas system', *Cell Res*, 24: 372-5.

Hall, V. J., and P. Hyttel. 2014. 'Breaking down pluripotency in the porcine embryo reveals both a premature and reticent stem cell state in the inner cell mass and unique expression profiles of the naive and primed stem cell states', *Stem Cells Dev*, 23: 2030-45.

Hao, Y., L. Lai, J. Mao*, et al.* 2004. 'Apoptosis in parthenogenetic preimplantation porcine embryos', *Biol Reprod*, 70: 1644-9.

Hart, A. H., L. Hartley, K. Sourris*, et al.* 2002. 'Mixl1 is required for axial mesendoderm morphogenesis and patterning in the murine embryo', *Development*, 129: 3597-608.

Hashimoto, M., Y. Yamashita, and T. Takemoto. 2016. 'Electroporation of Cas9 protein/sgRNA into early pronuclear zygotes generates non-mosaic mutants in the mouse', *Dev Biol*, 418: 1-9.

Hashimoto, Masakazu, and Tatsuya Takemoto. 2015. 'Electroporation enables the efficient mRNA delivery into the mouse zygotes and facilitates CRISPR/Cas9-based genome editing', *Scientific Reports*, 5: 11315.

Hassoun, R., P. Schwartz, K. Feistel*, et al.* 2009. 'Axial differentiation and early gastrulation stages of the pig embryo', *Differentiation*, 78: 301-11.

Hassoun, R., P. Schwartz, D. Rath*, et al.* 2010. 'Germ layer differentiation during early hindgut and cloaca formation in rabbit and pig embryos', *J Anat*, 217: 665-78.

Hayashi, K., S. M. de Sousa Lopes, and M. A. Surani. 2007. 'Germ cell specification in mice', *Science*, 316: 394-6.

Hayashi, K., H. Ohta, K. Kurimoto*, et al.* 2011. 'Reconstitution of the mouse germ cell specification pathway in culture by pluripotent stem cells', *Cell*, 146: 519-32.

Home, P., S. Ray, D. Dutta*, et al.* 2009. 'GATA3 Is Selectively Expressed in the Trophectoderm of Peri-implantation Embryo and Directly Regulates Cdx2 Gene Expression', *Journal of Biological Chemistry*, 284: 28729-37.

Hong, S. S., J. H. Choi, S. Y. Lee*, et al.* 2015. 'A Novel Small-Molecule Inhibitor Targeting the IL-6 Receptor beta Subunit, Glycoprotein 130', *J Immunol*, 195: 237-45.

Hou, L., Y. Srivastava, and R. Jauch. 2017. 'Molecular basis for the genome engagement by Sox proteins', *Semin Cell Dev Biol*, 63: 2-12.

Hsiau, Timothy, Travis Maures, Kelsey Waite*, et al.* 2018. 'Inference of CRISPR Edits from Sanger Trace Data', *bioRxiv*.

Hsu, P. D., D. A. Scott, J. A. Weinstein*, et al.* 2013. 'DNA targeting specificity of RNA-guided Cas9 nucleases', *Nat Biotechnol*, 31: 827-32.

Hudson, C., D. Clements, R. V. Friday*, et al.* 1997. 'Xsox17alpha and -beta mediate endoderm formation in Xenopus', *Cell*, 91: 397-405.

Igaz, P., S. Toth, and A. Falus. 2001. 'Biological and clinical significance of the JAK-STAT pathway; lessons from knockout mice', *Inflamm Res*, 50: 435-41.

Ip, Y. T., and T. Gridley. 2002. 'Cell movements during gastrulation: snail dependent and independent pathways', *Curr Opin Genet Dev*, 12: 423-9.

Irie, N., W. W. Tang, and M. Azim Surani. 2014. 'Germ cell specification and pluripotency in mammals: a perspective from early embryogenesis', *Reprod Med Biol*, 13: 203-15.

Irie, N., L. Weinberger, W. W. Tang*, et al.* 2015. 'SOX17 is a critical specifier of human primordial germ cell fate', *Cell*, 160: 253-68.

Jinek, Martin, Krzysztof Chylinski, Ines Fonfara*, et al.* 2012. 'A Programmable Dual-RNA–Guided DNA Endonuclease in Adaptive Bacterial Immunity', *Science*, 337: 816.

Julaton, V. T., and R. A. Reijo Pera. 2011. 'NANOS3 function in human germ cell development', *Hum Mol Genet*, 20: 2238-50.

Kanai-Azuma, M., Y. Kanai, J. M. Gad*, et al.* 2002. 'Depletion of definitive gut endoderm in Sox17-null mutant mice', *Development*, 129: 2367-79.

Kanai, Y., M. KanaiAzuma, T. Noce*, et al.* 1996. 'Identification of two Sox17 messenger RNA isoforms, with and without the high mobility group box region, and their differential expression in mouse spermatogenesis', *Journal of Cell Biology*, 133: 667-81.

Keller, R. 2005. 'Cell migration during gastrulation', *Curr Opin Cell Biol*, 17: 533-41.

Kerosuo, L., and M. Bronner-Fraser. 2012. 'What is bad in cancer is good in the embryo: importance of EMT in neural crest development', *Semin Cell Dev Biol*, 23: 320-32.

Kishigami, Satoshi, and Yuji Mishina. 2005. 'BMP signaling and early embryonic patterning'.

Kobayashi, T., H. Zhang, W. W. C. Tang*, et al.* 2017. 'Principles of early human development and germ cell program from conserved model systems', *Nature*, 546: 416-20.

Kojima, Y., K. Sasaki, S. Yokobayashi*, et al.* 2017. 'Evolutionarily Distinctive Transcriptional and Signaling Programs Drive Human Germ Cell Lineage Specification from Pluripotent Stem Cells', *Cell Stem Cell*, 21: 517-32 e5.

Koo, D. B., Y. K. Kang, J. S. Park*, et al.* 2004. 'A paucity of structural integrity in cloned porcine blastocysts produced in vitro', *Theriogenology*, 62: 779-89.

Kubaczka, C., F. Kaiser, and H. Schorle. 2017. 'Breaking the first lineage barrier - many roads to trophoblast stem cell fate', *Placenta*, 60 Suppl 1: S52-S56.

Kuijk, E. W., L. T. van Tol, H. Van de Velde*, et al.* 2012. 'The roles of FGF and MAP kinase signaling in the segregation of the epiblast and hypoblast cell lineages in bovine and human embryos', *Development*, 139: 871-82.

Kurosawa, H. 2007. 'Methods for inducing embryoid body formation: in vitro differentiation system of embryonic stem cells', *J Biosci Bioeng*, 103: 389-98.

Lamitina. T. (2007). Bacterial transformation. [Protocol]. Retrieved from: http://docs.wixstatic.com/ugd/803ab9_1ceb45bf208d4c59b75eed225d4414ff.pdf

Lawson, K. A., N. R. Dunn, B. A. J. Roelen*, et al.* 1999. 'Bmp4 is required for the generation of primordial germ cells in the mouse embryo', *Genes & Development*, 13: 424-36.

Lawson, K. A., and R. A. Pedersen. 1987. 'Cell Fate, Morphogenetic Movement and Population-Kinetics of Embryonic Endoderm at the Time of Germ Layer Formation in the Mouse', *Development*, 101: 627-52.

Lee, F. D. 1992. 'The role of interleukin-6 in development', *Dev Biol*, 151: 331-8.

Li, D. L., Z. W. Qiu, Y. J. Shao*, et al.* 2013. 'Heritable gene targeting in the mouse and rat using a CRISPR-Cas system', *Nature Biotechnology*, 31: 681-83.

Liang, P., Y. Xu, X. Zhang*, et al.* 2015. 'CRISPR/Cas9-mediated gene editing in human tripronuclear zygotes', *Protein Cell*, 6: 363-72.

Lu, R., A. Yang, and Y. Jin. 2011. 'Dual functions of T-box 3 (Tbx3) in the control of self-renewal and extraembryonic endoderm differentiation in mouse embryonic stem cells', *J Biol Chem*, 286: 8425-36.

Macháty, Zoltán, Billy N. Day, and Randall S. Prather. 1998. 'Development of Early Porcine Embryos In Vitro and In Vivo1', *Biology of Reproduction*, 59: 451-55.

Maeder, M. L., and C. A. Gersbach. 2016. 'Genome-editing Technologies for Gene and Cell Therapy', *Mol Ther*, 24: 430-46.

Martinez Barbera, J. P., M. Clements, P. Thomas*, et al.* 2000. 'The homeobox gene Hex is required in definitive endodermal tissues for normal forebrain, liver and thyroid formation', *Development*, 127: 2433.

Matsuda, T., T. Nakamura, K. Nakao*, et al.* 1999. 'STAT3 activation is sufficient to maintain an undifferentiated state of mouse embryonic stem cells', *EMBO J*, 18: 4261-9.

Menchero, S., T. Rayon, M. J. Andreu*, et al.* 2017. 'Signaling pathways in mammalian preimplantation development: Linking cellular phenotypes to lineage decisions', *Dev Dyn*, 246: 245-61.

Mitsunaga, S., J. Odajima, S. Yawata*, et al.* 2017. 'Relevance of iPSC-derived human PGC-like cells at the surface of embryoid bodies to prechemotaxis migrating PGCs', *Proc Natl Acad Sci U S A*, 114: E9913-E22.

Mitsunaga, S., and T. Shioda. 2018. 'Evolutionarily diverse mechanisms of germline specification among mammals: what about us?', *Stem Cell Investig*, 5: 12.

Mohamed, O. A., H. J. Clarke, and D. Dufort. 2004. 'Beta-catenin signaling marks the prospective site of primitive streak formation in the mouse embryo', *Dev Dyn*, 231: 416-24.

Momose, T., A. De Cian, K. Shiba*, et al.* 2018. 'High doses of CRISPR/Cas9 ribonucleoprotein efficiently induce gene knockout with low mosaicism in the hydrozoan Clytia hemisphaerica through microhomology-mediated deletion', *Sci Rep*, 8: 11734.

Murray, R., F. Lee, and C. P. Chiu. 1990. 'The genes for leukemia inhibitory factor and interleukin-6 are expressed in mouse blastocysts prior to the onset of hemopoiesis', *Mol Cell Biol*, 10: 4953-6.

Niemann, H., and D. Rath. 2001. 'Progress in reproductive biotechnology in swine', *Theriogenology*, 56: 1291-304.

Niemann, H., and C. Wrenzycki. 2000. 'Alterations of expression of developmentally important genes in preimplantation bovine embryos by in vitro culture conditions: implications for subsequent development', *Theriogenology*, 53: 21-34.

Niwa, H., Y. Toyooka, D. Shimosato*, et al.* 2005. 'Interaction between Oct3/4 and Cdx2 determines trophectoderm differentiation', *Cell*, 123: 917-29.

Nowotschin, S., I. Costello, A. Piliszek*, et al.* 2013. 'The T-box transcription factor Eomesodermin is essential for AVE induction in the mouse embryo', *Genes & Development*, 27: 997-1002.

Nüsslein-Volhard, Christiane. 1991. 'Determination of the embryonic axes of Drosophila', *Development*, 113: 1-10.

Ouimette, J. F., M. L. Jolin, A. L'Honore*, et al.* 2010. 'Divergent transcriptional activities determine limb identity', *Nat Commun*, 1: 35.

Paffoni, A., T. A. Brevini, F. Gandolfi*, et al.* 2008. 'Parthenogenetic activation: biology and applications in the ART laboratory', *Placenta*, 29 Suppl B: 121-5.

Papaioannou, V. E. 2001. 'T-box genes in development: from hydra to humans', *Int Rev Cytol*, 207: 1-70.

Papaioannou, V. E. 2014. 'The T-box gene family: emerging roles in development, stem cells and cancer', *Development*, 141: 3819-33.

Papatsenko, D., A. Waghray, and I. R. Lemischka. 2018. 'Feedback control of pluripotency in embryonic stem cells: Signaling, transcription and epigenetics', *Stem Cell Res*, 29: 180-88.

Pattanayak, V., S. Lin, J. P. Guilinger*, et al.* 2013. 'High-throughput profiling of off-target DNA cleavage reveals RNA-programmed Cas9 nuclease specificity', *Nat Biotechnol*, 31: 839-43.

Peng, G., and N. Jing. 2017. 'The genome-wide molecular regulation of mouse gastrulation embryo', *Sci China Life Sci*, 60: 363-69.

Pevny, L. H., and R. LovellBadge. 1997. 'Sox genes find their feet', *Current Opinion in Genetics & Development*, 7: 338-44.

Picozzi, Paola, Fengxiang Wang, Kevin Cronk*, et al.* 2009. 'Eomesodermin Requires Transforming Growth Factor-β/Activin Signaling and Binds Smad2 to Activate Mesodermal Genes', *Journal of Biological Chemistry*, 284: 2397-408.

Posfai, E., S. Petropoulos, F. R. O. de Barros*, et al.* 2017. 'Position- and Hippo signaling-dependent plasticity during lineage segregation in the early mouse embryo', *eLife*, 6: e22906.

Pulina, M. V., K. E. Sahr, S. Nowotschin*, et al.* 2014. 'A conditional mutant allele for analysis of Mixl1 function in the mouse', *Genesis*, 52: 417-23.

Qin, W., S. L. Dion, P. M. Kutny*, et al.* 2015. 'Efficient CRISPR/Cas9-Mediated Genome Editing in Mice by Zygote Electroporation of Nuclease', *Genetics*, 200: 423-30.

Ralston, A., and J. Rossant. 2008. 'Cdx2 acts downstream of cell polarization to cell-autonomously promote trophectoderm fate in the early mouse embryo', *Dev Biol*, 313: 614-29.

Ramos-Ibeas, Priscila, Fei Sang, Qifan Zhu*, et al.* 2018. 'Lineage segregation, pluripotency and X-chromosome inactivation in the pig pre-gastrulation embryo', *bioRxiv*.

Rawlings, J. S., K. M. Rosler, and D. A. Harrison. 2004. 'The JAK/STAT signaling pathway', *J Cell Sci*, 117: 1281-3.

Rivera-Perez, J. A., and T. Magnuson. 2005. 'Primitive streak formation in mice is preceded by localized activation of Brachyury and Wnt3', *Dev Biol*, 288: 363-71.

Rodda, D. J., J. L. Chew, L. H. Lim*, et al.* 2005. 'Transcriptional regulation of nanog by OCT4 and SOX2', *J Biol Chem*, 280: 24731-7.

Russ, A. P., S. Wattler, W. H. Colledge*, et al.* 2000. 'Eomesodermin is required for mouse trophoblast development and mesoderm formation', *Nature*, 404: 95-9.

Ryan, K., N. Garrett, A. Mitchell*, et al.* 1996. 'Eomesodermin, a key early gene in Xenopus mesoderm differentiation', *Cell*, 87: 989-1000.

Saitou, M., S. C. Barton, and M. A. Surani. 2002. 'A molecular programme for the specification of germ cell fate in mice', *Nature*, 418: 293-300.

Saitou, M., and M. Yamaji. 2012. 'Primordial germ cells in mice', *Cold Spring Harb Perspect Biol*, 4.

Sansone, P., and J. Bromberg. 2012. 'Targeting the interleukin-6/Jak/stat pathway in human malignancies', *J Clin Oncol*, 30: 1005-14.

Shen, X. H., X. S. Cui, S. H. Lee*, et al.* 2012. 'Interleukin-6 Enhances Porcine Parthenote Development In Vitro, through the IL-6/Stat3 Signaling Pathway', *Journal of Reproduction and Development*, 58: 453-60.

Solnica-Krezel, L., and D. S. Sepich. 2012. 'Gastrulation: making and shaping germ layers', *Annu Rev Cell Dev Biol*, 28: 687-717.

Stemple, D. L. 2001. 'Vertebrate development: the subtle art of germ-layer specification', *Curr Biol*, 11: R878-81.

Stower, M. J., and F. Bertocchini. 2017. 'The evolution of amniote gastrulation: the blastopore-primitive streak transition', *Wiley Interdiscip Rev Dev Biol*, 6: e262.

Sugawa, F., M. J. Arauzo-Bravo, J. Yoon*, et al.* 2015. 'Human primordial germ cell commitment in vitro associates with a unique PRDM14 expression profile', *EMBO J*, 34: 1009-24.

Suzuki, Akio S., Koji Sakaguchi, Mineko Katagiri*, et al.* 2002. 'Blastopore formation and dorsal mesoderm induction are independent events in early Cynops embryogenesis', *Development, Growth and Differentiation*, 44: 303-13.

Swarr, D. T., and E. E. Morrisey. 2015. 'Lung endoderm morphogenesis: gasping for form and function', *Annu Rev Cell Dev Biol*, 31: 553-73.

Tai, C. I., E. N. Schulze, and Q. L. Ying. 2014. 'Stat3 signaling regulates embryonic stem cell fate in a dose-dependent manner', *Biol Open*, 3: 958-65.

Takeda, K., K. Noguchi, W. Shi*, et al.* 1997. 'Targeted disruption of the mouse Stat3 gene leads to early embryonic lethality', *Proc Natl Acad Sci U S A*, 94: 3801-4.

Talbot, J. C., and Amacher, S.L. (2014) A Streamlined CRISPR Pipeline to Reliably Generate Zebrafish Frameshifting Alleles. Zebrafish. 11(6), pg. 583-585

Tam, P. P., and R. R. Behringer. 1997. 'Mouse gastrulation: the formation of a mammalian body plan', *Mech Dev*, 68: 3-25.

Tam, P. P., and D. A. Loebel. 2007. 'Gene function in mouse embryogenesis: get set for gastrulation', *Nat Rev Genet*, 8: 368-81.

Tang, L., Y. Zeng, H. Du*, et al.* 2017. 'CRISPR/Cas9-mediated gene editing in human zygotes using Cas9 protein', *Mol Genet Genomics*, 292: 525-33.

Tang, W. W., S. Dietmann, N. Irie*, et al.* 2015. 'A Unique Gene Regulatory Network Resets the Human Germline Epigenome for Development', *Cell*, 161: 1453-67.

Tao, L., M. Yang, X. Wang*, et al.* 2016. 'Efficient biallelic mutation in porcine parthenotes using a CRISPR-Cas9 system', *Biochem Biophys Res Commun*, 476: 225-29.

Twyman, Richard M. 2001. 'Instant notes, developmental biology'. Bios Scientific.

Uemura, M., K. Hara, H. Shitara*, et al.* 2010. 'Expression and function of mouse Sox17 gene in the specification of gallbladder/bile-duct progenitors during early foregut morphogenesis', *Biochem Biophys Res Commun*, 391: 357-63.

Valdez Magana, G., A. Rodriguez, H. Zhang*, et al.* 2014. 'Paracrine effects of embryo-derived FGF4 and BMP4 during pig trophoblast elongation', *Dev Biol*, 387: 15-27.

van Boxtel, A. L., A. D. Economou, C. Heliot*, et al.* 2018. 'Long-Range Signaling Activation and Local Inhibition Separate the Mesoderm and Endoderm Lineages', *Dev Cell*, 44: 179-91 e5.

van de Ven, C., M. Bialecka, R. Neijts*, et al.* 2011. 'Concerted involvement of Cdx/Hox genes and Wnt signaling in morphogenesis of the caudal neural tube and cloacal derivatives from the posterior growth zone', *Development*, 138: 3451-62.

Viotti, M., S. Nowotschin, and A. K. Hadjantonakis. 2014. 'SOX17 links gut endoderm morphogenesis and germ layer segregation', *Nat Cell Biol*, 16: 1146-56.

Wang, H., H. Yang, C. S. Shivalila*, et al.* 2013. 'One-step generation of mice carrying mutations in multiple genes by CRISPR/Cas-mediated genome engineering', *Cell*, 153: 910-8.

Wegner, M. 2010. 'All purpose Sox: The many roles of Sox proteins in gene expression', *Int J Biochem Cell Biol*, 42: 381-90.

Wicklow, E., S. Blij, T. Frum*, et al.* 2014. 'HIPPO pathway members restrict SOX2 to the inner cell mass where it promotes ICM fates in the mouse blastocyst', *PLoS Genet*, 10: e1004618.

Winnier, G., M. Blessing, P. A. Labosky*, et al.* 1995. 'Bone Morphogenetic Protein-4 Is Required for Mesoderm Formation and Patterning in the Mouse', *Genes & Development*, 9: 2105-16.

Withington, S., R. Beddington, and J. Cooke. 2001. 'Foregut endoderm is required at head process stages for anteriormost neural patterning in chick', *Development*, 128: 309-20.

Wu, Q., X. Chen, J. Zhang*, et al.* 2006. 'Sall4 interacts with Nanog and co-occupies Nanog genomic sites in embryonic stem cells', *J Biol Chem*, 281: 24090-4.

Yamaguchi, M., M. Michishita, K. Hirayoshi*, et al.* 1992. 'Down-regulation of interleukin 6 receptors of mouse myelomonocytic leukemic cells by leukemia inhibitory factor', *J Biol Chem*, 267: 22035-42.

Yan, B., J. J. Wei, Y. Yuan*, et al.* 2013. 'IL-6 cooperates with G-CSF to induce protumor function of neutrophils in bone marrow by enhancing STAT3 activation', *J Immunol*, 190: 5882-93.

Yang, H., H. Wang, C. S. Shivalila*, et al.* 2013. 'One-step generation of mice carrying reporter and conditional alleles by CRISPR/Cas-mediated genome engineering', *Cell*, 154: 1370-9.

Yen, S. T., M. Zhang, J. M. Deng*, et al.* 2014. 'Somatic mosaicism and allele complexity induced by CRISPR/Cas9 RNA injections in mouse zygotes', *Dev Biol*, 393: 3-9.

Yi, Y. J., and C. S. Park. 2005. 'Parthenogenetic development of porcine oocytes treated by ethanol, cycloheximide, cytochalasin B and 6-dimethylaminopurine', *Anim Reprod Sci*, 86: 297-304.

Zernicka-Goetz, M. 2002. 'Patterning of the embryo: the first spatial decisions in the life of a mouse', *Development*, 129: 815-29.

Zhao, D., X. Feng, X. Zhu*, et al.* 2017. 'CRISPR/Cas9-assisted gRNA-free one-step genome editing with no sequence limitations and improved targeting efficiency', *Sci Rep*, 7: 16624.

Zhou, J., J. Wang, B. Shen*, et al.* 2014. 'Dual sgRNAs facilitate CRISPR/Cas9-mediated mouse genome targeting', *FEBS J*, 281: 1717-25.

Zhu, X., Y. Xu, S. Yu*, et al.* 2014. 'An efficient genotyping method for genome-modified animals and human cells generated with CRISPR/Cas9 system', *Sci Rep*, 4: 6420.

Ziomek, C. A., and M. H. Johnson. 1980. 'Cell-Surface Interaction Induces Polarization of Mouse 8-Cell Blastomeres at Compaction', *Cell*, 21: 935-42.

Zuo, E., Y. J. Cai, K. Li*, et al.* 2017. 'One-step generation of complete gene knockout mice and monkeys by CRISPR/Cas9-mediated gene editing with multiple sgRNAs', *Cell Res*, 27: 933-45.